

Constraints on T-Odd, P-Even Interactions from Electric Dipole Moments, Revisited

A. Kurylov¹, G. C. McLaughlin^{2,4}, and M.J. Ramsey-Musolf^{1,3}

¹ Department of Physics, University of Connecticut, Storrs, CT 06269 USA

² Department of Physics and Astronomy, State University of New York, Stony Brook, NY 11794 USA

³ Theory Group, Thomas Jefferson National Accelerator Facility, Newport News, VA 23606 USA

⁴ Previous address: TRIUMF, 4004 Wesbrook Mall, Vancouver, B.C. Canada V6T2A3

Abstract

We construct the relationship between nonrenormalizable, effective, time-reversal violating (TV) parity-conserving (PC) interactions of quarks and gauge bosons and various low-energy TVPC and TV parity-violating (PV) observables. Using effective field theory methods, we delineate the scenarios under which experimental limits on permanent electric dipole moments (EDM's) of the electron, neutron, and neutral atoms as well as limits on TVPC observables provide the most stringent bounds on new TVPC interactions. Under scenarios in which parity invariance is restored at short distances, the one-loop EDM of elementary fermions generate the most severe constraints. The limits derived from the atomic EDM of ¹⁹⁹Hg are considerably weaker. When parity symmetry remains broken at short distances, direct TVPC search limits provide the least ambiguous bounds. The direct limits follow from TVPC interactions between two quarks.

1 Introduction

The search for physics beyond the Standard Model (SM) is a topic of considerable interest in high-energy particle physics. Concurrently, efforts are also underway to uncover signatures of new physics at low- and medium-energies using atomic and nuclear processes. In this respect, there exist tantalizing hints of new physics in results of neutron and superallowed nuclear β -decays, which imply a value for $|V_{ud}|$ differing from the SM unitarity requirement by two or more σ [1]. Similarly, the weak charge of the cesium atom, Q_w , measured in atomic parity-violation (APV) by the Boulder group, has been found to differ from the SM prediction by 2.5σ [2] (See, however, Ref. [3]). If conventional many-body atomic and nuclear effects can be ruled out as the source of these deviations, the β -decay and APV results imply the existence of new physics at the 1-10 TeV scale[4, 5]. This possibility has motivated a variety of additional atomic and nuclear new physics searches, including new measurements of the neutron β -decay parameters, APV observables along a chain of isotopes, and parity-violating (PV) electron-electron and electron-proton scattering.

One possible manifestation of new physics not probed by the aforementioned experiments would be the existence of new low-energy interactions involving a single generation of fermions which violate time-reversal invariance (T) but conserve parity invariance (P). Such interactions are allowed in the SM when quarks of different generations participate. Recently, the first non-zero result for a $\Delta S = 1$ T-violating, P-conserving (TVPC) observable has been reported by the CPLEAR Collaboration, which measured the $K^0 - \bar{K}^0$ decay asymmetry [6]. The results are consistent with the value expected from the measured CP-violating parameter ϵ and the CPT theorem. No new physics is required to explain this result. In the $\Delta S = 0$ sector, a variety of direct searches for TVPC effects have been carried out. These efforts include studies of detailed balance in nuclear reactions[7], γ -ray correlations in nuclear γ -decay[8], five-fold correlations (FC) in the scattering of epithermal neutrons from aligned nuclear targets[10, 11], charge symmetry breaking (CSB) in np scattering [12, 13, 14], and the $\vec{J} \cdot (\hat{p}_e \times \hat{p}_\nu)$ in neutron β -decay[15]. Thus far, all studies have yielded null results. The limits from the purely hadronic reactions imply $\alpha_T \lesssim \text{few} \times 10^{-3}$, where α_T gives the ratio of TVPC nuclear matrix elements to those of the residual strong interaction.

Limits on $\Delta S = 0$ TVPC interactions involving light quarks may also be derived indirectly from results for atomic, neutron, and electron electric dipole moments (EDM's). As observed in Ref. [16], the presence of both a new TVPC interaction and a conventional PV interaction (*e.g.*, in the Standard Model) could conspire to generate a non-zero EDM, whose interaction with an external field violates both P and T. To the extent that PV radiative corrections to possible new TVPC interactions can be calculated, one can derive limits on new TVPC interactions from EDM results. Attempts to do so were first reported in Ref. [16]. The calculation involved two external elementary fermions (*e.g.*, two valence quarks in the neutron) and a one-loop Z -boson radiative correction to dimension seven, four-fermion, TVPC operators. Two-loop effects, involving a single external fermion, for the electron EDM, d_e , and neutron EDM, d_n , were later studied in Ref. [17]. Naïvely, one might expect the most stringent bounds on new TVPC interactions to be derived at one-loop order from the experimental limit on the atomic electric dipole moment of mercury, $d_A(^{199}\text{Hg})$, since the latter is nearly two orders of magnitude more severe than the bound on d_n . It was argued in Ref. [17], however, that the two-loop effects in d_e and d_n generate considerably more stringent bounds than do the results of d_A . Subsequently, the authors of Ref. [18] recast the analysis of Refs. [16, 17] into the framework of low-energy effective field theory (EFT). It was argued in Ref. [18] that the results of Ref. [17] imply bounds on new TVPC interactions in excess of those presently achievable with direct TVPC searches by several orders of magnitude. These conclusions have had a discouraging effect on further direct TVPC searches.

Recently, it was argued that the conclusions of Ref. [17] are inconsistent with the separation of scales underlying EFT [20]. In brief, the argument is as follows[21]. Let Λ_{TVPC} denote the mass scale below which use of an EFT involving nonrenormalizable TVPC operators makes sense. One may expand the EDM of an elementary particle, neutron, or atom as

$$d = \beta_5 C_5 \frac{1}{\Lambda_{TVPC}} + \beta_6 C_6 \frac{M}{\Lambda_{TVPC}^2} + \beta_7 C_7 \frac{M^2}{\Lambda_{TVPC}^3} + \dots \quad , \quad (1)$$

where the C_d denote the set of *a priori* unknown coefficients of dimension d nonrenormalizable operators in the effective Lagrangian, the β_d are calculable quantities arising from loops or many-body matrix elements, and $M < \Lambda_{TVPC}$ is a mass scale associated with the appropriate dynamical degree of freedom in the EFT. The C_d parameterize one's ignorance about the short-distance

($p \gtrsim \Lambda_{TVPC}$) dynamics of the new time-reversal violating physics. The first contributions from new TVPC interactions appear in the C_7 .

One may now consider Eq. (1) under two scenarios:

Scenario (A) Parity symmetry is restored at some scale $\mu \lesssim \Lambda_{TVPC}$. In this case, all of the coefficients C_5 and C_6 must vanish at tree-level in the EFT since parity invariance holds at short distances. Consequently, the first contributions to the EDM arise from loops involving the TVPC C_7 operators. Since $M/\Lambda_{TVPC} < 1$, these contributions presumably dominate the remaining terms in the series. Hence, one may use experimental EDM limits to constrain C_7/Λ_{TVPC}^3 . As shown below, the limits obtained from EDM's under this scenario vastly exceed those obtainable from direct searches.

Scenario (B) Parity symmetry is restored at $\mu \gtrsim \Lambda_{TVPC}$. In this case, the C_5 and C_6 do not, in general, vanish at tree-level in the EFT since both PV and TV interactions take place at short distance. There exists no reason to assume they fail to conspire in generating the lowest dimension TVPV effective interactions. Consequently, the TVPC interactions do not generate the leading contribution to the EDM as in Scenario (A). Without independent information on the $C_{5,6}$ one cannot use the EDM as a direct handle on the TVPC C_7 terms. The latter may be more or less suppressed relative to the lower dimension contributions depending on the size of M/Λ_{TVPC} . Since one has no *a priori* information on M/Λ_{TVPC} , one can say very little about the importance of TVPC contributions. For the sake of argument, one might assume $M/\Lambda_{TVPC} \ll 1$ so that the first term in Eq. (1) dominates. In this case, the low-energy effects of TVPC interactions would be negligible. In the more general situation, however, one would have to use direct TVPC searches to constrain the new TVPC interactions under this scenario.

The analysis of Refs. [17, 16] implicitly assumes Scenario (A). The EDM calculations performed by these authors, however, do not display the proper $1/\Lambda_{TVPC}^3$ scaling behavior which follows from EFT. The reasons for this failure are discussed in Ref. [20] and summarized below. It was also shown in Ref. [20] that there exist additional TVPC operators, not considered in Refs. [16, 17, 18], which contribute to the elementary fermion EDM at one-loop order. Under Scenario (A), these one loop effects yield the most stringent constraints on the size of TVPC effects.

In what follows, we extend the analysis of Ref. [20] to include many-quark TVPC contributions to the neutron EDM – first studied in Ref. [16] – and

to atomic EDM's. We concentrate on Scenario (A), since under Scenario (B) one cannot use EDM's to derive unambiguous information about TVPC new physics. In the case of the neutron EDM, we complete the one-loop analysis of Ref. [16], including additional diagrams required by electromagnetic gauge invariance. We show that the impact of these new diagrams is as large as the one-loop effects considered previously in Ref. [16]. We also compute tree-level contributions arising from dimension seven TVPC operators not considered in Ref. [16].

In the case of atomic EDM's, we consider the situation in which they arise from purely hadronic TVPC interactions in the nucleus. Traditionally, the effects of non-leptonic T-violation in nuclear and atomic processes have been analyzed using collective degrees of freedom (mesons and baryons), rather than fundamental quark-quark or quark-gluon interactions. The T-violating effects are characterized by hadronic coupling constants which may be related to the underlying quark and gluon T-violating interactions using standard hadron structure techniques. In this context, two hadronic effects are of interest: (a) the presence of a purely TVPC meson-nucleon interaction and (b) the presence of a TVPV meson-nucleon interaction.

The leading “long-range” TVPC effect arises from ρ -meson exchange, where the TVPC ρNN vertex is characterized by a coupling strength \bar{g}_ρ and an interaction [19]

$$\mathcal{L}_{\rho NN}^{TVPC} = i\sqrt{2}\bar{g}_\rho f_\rho \frac{\kappa_V}{2m_n} \bar{N} \sigma^{\mu\lambda} (\tau^- \partial_\lambda \rho_\mu^+ - \tau^+ \partial_\lambda \rho_\mu^-) N \quad , \quad (2)$$

where $f_\rho = 2.79$ and $\kappa_V = 3.70$. A time-reversal violating parity violating (TVPV) nuclear effect arises when the second vertex in the exchange is parity-violating. Alternately, a TVPV atomic moment can be generated by a TVPC nuclear ρ -exchange and the PV exchange of a Z -boson between the nucleus and atomic electrons (see Fig. 1).

Similarly, the longest-range TVPV effects generally arise from π -exchange. In this case, the relevant TVPV πNN couplings are $\bar{g}_\pi^{(I)'}$, where the superscript denotes the isospin channel and correspond to the interactions

$$\begin{aligned} \mathcal{L}_{\pi NN}^{TVPV} = & \bar{N} \left[\bar{g}_\pi^{(0)'} \vec{\tau} \cdot \vec{\pi} + \bar{g}_\pi^{(1)'} \pi^0 \right. \\ & \left. + \bar{g}_\pi^{(2)'} (3\tau_z \pi^0 - \vec{\tau} \cdot \vec{\pi}) \right] N \end{aligned} \quad (3)$$

Non-zero values of $\bar{g}_\pi^{(I)'}$ may arise from either new TVPC interactions plus weak radiative corrections, or from more conventional TVPV interactions, such as the θ -term in the QCD Lagrangian. The latter have been considered extensively elsewhere [19], and we concentrate on the former.

Upper bounds on $|\bar{g}_\rho|$ have been derived from a variety of T-violating, P-conserving experiments, including the studies of detailed balance in nuclear reactions[7], neutron transmission through an aligned ^{165}Ho target[10], and CSB terms in the np scattering cross section[12]. In addition, measurements of d_n and d_A yield bounds on \bar{g}_ρ , when PV and TVPC interactions conspire to generate an EDM. Under Scenario (A), the EDM limits on \bar{g}_ρ may be stronger than those obtained from TVPC nuclear processes[27]. Regarding the $\bar{g}_\pi^{(I)'}$, experimental EDM limits yield the most stringent bounds. As discussed in detail in Ref. [19], d_n and $d_A(^{199}\text{Hg})$ are sensitive to different linear combinations of the $\bar{g}_\pi^{(I)'}$. Roughly speaking, the EDM upper bounds on the $|\bar{g}_\pi^{(I)'}|$ are of the order of a few $\times 10^{-11}$.

In this paper, we relate \bar{g}_ρ and the $\bar{g}_\pi^{(I)'}$ to the underlying TVPC quark and gluon operators, and use limits on the hadronic couplings to infer limits on these underlying interactions. We then compare these limits as well as those obtained from the one-loop many-quark contributions to d_n with those obtained from the EDM's of elementary fermions as in Ref. [20]. We find:

1. Under Scenario (A), the one-loop elementary fermion EDM studied in Ref. [20] produces the most stringent limits on new TVPC interactions when applied to the electron and neutron. Many-quark effects d_n or d_A are suppressed by at least five orders of magnitude.
2. By making certain naturalness assumptions, one may use experimental EDM limits to derive lower bounds on Λ_{TVPC} . Under Scenario (A), one infers from d_e (single-quark d_n) limits that $\Lambda_{TVPC} \gtrsim 260$ TeV (~ 110 TeV) if the new TVPC physics is strong. The corresponding bounds derived from many-quark effects in d_n and $d_A(^{199}\text{Hg})$ are at roughly 1000 times weaker. In order for $d_A(^{199}\text{Hg})$ to provide competitive limits, the precision of the atomic EDM experiments would need to improve by roughly nine orders of magnitude¹.
3. Under Scenario (A), one expects $\alpha_T \lesssim 10^{-15}$.

¹However, at some point, improved precision in d_A would improve tighten the bounds on d_n .

4. For Scenario (B), experimental limits on \bar{g}_ρ derived from FC in neutron transmission and CSB in np scattering produce the strongest limits on TVPC new physics. In terms of mass scales, these limits give $\Lambda_{TVPC} \gtrsim 1$ GeV for new strong TVPC physics. An improvement of six orders of magnitude in experimental precision would bring this lower bound up to the weak scale.

The analysis leading to these conclusions is presented in the remainder of the paper as follows. In section 2, we review the framework of EFT for new low-energy TVPC and TVPV interactions. In section 3 we illustrate the application of this framework by considering the EDM of an elementary fermion, as discussed in Ref. [20]. In section 4, we discuss the renormalization of effective TVPV four-fermion operators arising from PV radiative corrections to effective TVPC interactions. Here, we take particular care to implement electromagnetic gauge invariance. The latter implies the existence of additional contributions to the EDM's of composite systems not considered in Ref. [16]. In section 5, we relate the effective TVPC and TVPV operators to \bar{g}_ρ and the $\bar{g}_\pi^{(I)'}$, respectively, using the quark model, factorization, and current algebra. We also compute new many-quark contributions to d_n generated by new operators – including those required by gauge invariance – not considered in Ref. [16]. In section 6, we compare the implications of the many-quark contributions for the scale of new TVPC interactions with those obtained from the study of Ref. [20]. We also consider the limits on \bar{g}_ρ and the $\bar{g}_\pi^{(I)'}$ obtained from atomic EDM limits and direct searches and the corresponding implications for new TVPC interactions under the two scenarios outlined above. Section 6 summarizes our conclusions.

2 Effective field theory and new TVPC interactions

Herczeg *et al* have shown that TVPC interactions between quarks cannot arise from tree-level boson exchange in renormalizable gauge theories [9]. Such interactions could, however, be generated by higher-order or non-perturbative effects. Whatever new physics produces P-conserving T-violation among light quarks and gluons must be characterized by some heavy mass scale, Λ_{TVPC} . Given that the underlying renormalizable gauge theory for P-conserving

T-violation is not known, it is natural to consider the low-energy consequences of such a theory in the context of an EFT valid below the scale Λ_{TVPC} . Letting \mathcal{L}_{NEW} denote the effective, low-energy Lagrangian for new physics, we follow Ref. [18] and expand in inverse powers of Λ_{TVPC} :

$$\mathcal{L}_{NEW} = \mathcal{L}_4 + \frac{1}{\Lambda_{TVPC}} \mathcal{L}_5 + \frac{1}{\Lambda_{TVPC}^2} \mathcal{L}_6 + \frac{1}{\Lambda_{TVPC}^3} \mathcal{L}_7 + \dots \quad , \quad (4)$$

where the subscripts denote the dimension of the operators appearing in each term and where

$$\mathcal{L}_d = \sum_k C_d^k \mathcal{O}_d^k \quad (5)$$

with the sum running over k complete set of dimension d operators $\{\mathcal{O}_d^k\}$. The lowest dimension T-violating operators appear in \mathcal{L}_5 . These operators are TVPV only. Of particular interest here are the electric dipole fermion-gauge boson interactions:

$$\mathcal{O}_5^{f\gamma} = -\frac{i}{2} \bar{\psi}_f \sigma_{\mu\nu} \gamma_5 \psi_f F^{\mu\nu} \quad (6)$$

$$\mathcal{O}_5^{fZ} = -\frac{i}{2} \bar{\psi}_f \sigma_{\mu\nu} \gamma_5 \psi_f Z^{\mu\nu} \quad (7)$$

$$\mathcal{O}_5^{fg} = -\frac{i}{2} \bar{\psi}_f \sigma_{\mu\nu} \gamma_5 \lambda^a \psi_f G^{a\ \mu\nu} \quad , \quad (8)$$

where $F^{\mu\nu}$, $Z^{\mu\nu}$, and $G^{a\ \mu\nu}$ denote the photon, Z-boson, and gluon field strength tensors, respectively, and the λ^a are the Gell-Mann matrices.

The term \mathcal{L}_6 contains the lowest-order TVPV four-fermion operators, which include

$$\mathcal{O}_{6a}^{ff'} = i \bar{\psi}_f \psi_f \bar{\psi}_{f'} \gamma_5 \psi_{f'} \quad (9)$$

$$\mathcal{O}_{6b}^{ff'} = i \bar{\psi}_f \lambda^a \psi_f \bar{\psi}_{f'} \lambda^a \gamma_5 \psi_{f'} \quad (10)$$

$$\mathcal{O}_{6c}^{ff'} = i \bar{\psi}_f \sigma_{\mu\nu} \psi_f \bar{\psi}_{f'} \sigma^{\mu\nu} \gamma_5 \psi_{f'} \quad (11)$$

$$\mathcal{O}_{6d}^{ff'} = i \bar{\psi}_f \lambda^a \sigma_{\mu\nu} \psi_f \bar{\psi}_{f'} \lambda^a \sigma^{\mu\nu} \gamma_5 \psi_{f'} \quad (12)$$

and so forth.

The lowest-dimension TVPC interactions arise in \mathcal{L}_7 . Here, we consider the following three:

$$\mathcal{O}_{7a}^{ff'} = i \bar{\psi}_f \gamma_5 \sigma_{\mu\nu} (\overleftrightarrow{D}_\nu + \overleftrightarrow{D}_\nu) \psi_f \bar{\psi}_{f'} \gamma^\mu \gamma_5 \psi_{f'} + \text{h.c.} \quad (13)$$

$$\mathcal{O}_{7b}^{g\gamma} = \bar{\psi}_f \sigma_{\mu\nu} \lambda_a \psi_f G_a^{\mu\alpha} F_\alpha^\nu \quad (14)$$

$$\mathcal{O}_{7c}^{Z\gamma} = \bar{\psi}_f \sigma_{\mu\nu} \psi_f Z^{\mu\alpha} F_\alpha^\nu \quad . \quad (15)$$

The operator $\mathcal{O}_{7a}^{ff'}$ was first considered in Refs. [16, 17], while $\mathcal{O}_{7b}^{g\gamma}$ was introduced in Ref. [18]. The interaction $\mathcal{O}_{7c}^{Z\gamma}$ was subsequently considered in Ref. [20].

The $d = 7$ Lagrangian also contains several TVPV operators. Among those relevant to us are

$$\mathcal{O}_{7d}^{ff'} = \bar{\psi}_f \gamma^\mu (\overleftarrow{D}_\mu - \overrightarrow{D}_\mu) \psi_f \bar{\psi}_{f'} \gamma_5 \psi_{f'} \quad (16)$$

$$\mathcal{O}_{7e}^{ff'} = \bar{\psi}_f \psi_f \bar{\psi}_{f'} \gamma^\mu \gamma_5 (\overleftarrow{D}_\mu + \overrightarrow{D}_\mu) \psi_{f'} \quad (17)$$

$$\mathcal{O}_{7f}^{ff'} = i \bar{\psi}_f \gamma^\nu \psi_f \bar{\psi}_{f'} \sigma_{\mu\nu} \gamma_5 (\overleftarrow{D}_\mu + \overrightarrow{D}_\mu) \psi_{f'} \quad (18)$$

$$\mathcal{O}_{7g}^{ff'} = i \bar{\psi}_f \gamma^\nu \gamma_5 \psi_f \bar{\psi}_{f'} \sigma_{\mu\nu} (\overleftarrow{D}_\mu - \overrightarrow{D}_\mu) \psi_{f'} \quad (19)$$

$$\mathcal{O}_{7h}^{ff'} = \bar{\psi}_f \gamma^\mu \psi_f \bar{\psi}_{f'} \gamma_5 (\overleftarrow{D}_\mu - \overrightarrow{D}_\mu) \psi_{f'} \quad (20)$$

$$\mathcal{O}_{7i}^{ff'} = i \bar{\psi}_f \gamma^\mu (\overleftarrow{D}^\nu + \overrightarrow{D}^\nu) \psi_f \bar{\psi}_{f'} \sigma_{\mu\nu} \gamma_5 \psi_{f'} \quad (21)$$

$$\mathcal{O}_{7j}^{ff'} = i \bar{\psi}_f \gamma^\nu \gamma_5 (\overleftarrow{D}_\mu - \overrightarrow{D}_\mu) \psi_f \bar{\psi}_{f'} \sigma_{\mu\nu} \psi_{f'} \quad (22)$$

The specific forms of other $d \geq 5$ TVPV operators and $d \geq 7$ TVPC operators are not relevant to the present discussion, so we do not list them explicitly.

A key ingredient underlying the expansion of Eq. (4) is a separation of scales and an associated power-counting scheme. Specifically, the contribution to a T-violating observable from any physics associated with scales $\mu \gtrsim \Lambda_{TVPC}$ is contained in the operator coefficients, C_d . These short-distance contributions are not calculable since the underlying theory (*e.g.*, renormalizable gauge theory) responsible for TVPC effects is not known². Consequently, the C_d can only be determined from experiment. Contributions from physics having $\mu < \Lambda_{TVPC}$ live in loops and many-body (*e.g.*, hadronic) matrix elements containing the non-renormalizable operators \mathcal{O}_d and physical degrees of freedom having masses and momenta less than the scale Λ_{TVPC} . Only these “long-distance” contributions can be computed using the EFT.

As a consequence of this scale separation, one obtains a systematic power-counting scheme by which to organize contributions to any low-energy T-violating observable. If d is the lowest dimension of an effective operator which contributes to such an observable \mathcal{A}^{T-ODD} , then

$$\mathcal{A}^{T-ODD} \sim C_d \left(\frac{p}{\Lambda_{TVPC}} \right)^{d-4} + \dots \quad , \quad (23)$$

²If this underlying theory were known, one would have no need to employ the expansion in Eq. (4) in the first place

where p denotes a mass or momentum smaller than Λ_{TVPC} . To the extent that $p \ll \Lambda_{TVPC}$, contributions from higher-dimension operators will be suppressed relative to those from \mathcal{O}_d by powers of (p/Λ_{TVPC}) . In general, one may thus truncate the expansion of \mathcal{A}^{T-ODD} at the first or first few orders in (p/Λ_{TVPC}) . In our analysis of the EDM, we find p is one of the following: elementary fermion mass, m_f ; weak gauge boson mass, M_Z ; QCD scale, Λ_{QCD} ; inverse hadron size, $1/r_{HAD}$; and long wavelength photon momentum, q .

Any renormalization of the \mathcal{O}_d by loops involving any one of the \mathcal{O}_d and, *e.g.*, degrees of freedom appearing in \mathcal{L}_4 must be carried out in a manner which preserves the EFT scale separation. In particular, only intermediate states with momenta and energies below Λ_{TVPC} must contribute to loop integrals. Higher-momentum ($p \gtrsim \Lambda_{TVPC}$) states have been effectively integrated out in arriving at the expansion in Eq. (4). Consequently, we regulate all loop integrals using dimensional regularization (DR), which preserves the separation of scales. Since the subtraction scale μ arising in DR only appears logarithmically in any regulated amplitude and never as a power, the use of DR does not alter the EFT power counting described above. We emphasize that the cut-off regulator used in Refs. [16, 17] does not preserve the EFT scale separation. In those analyses, loop integrals were cut off at momenta $p \sim \Lambda_{TVPC}$. Consequently, in Refs. [16, 17] the renormalization of the EDM \mathcal{O}_{5a} due to loops involving any $d > 5$ operator scales as $1/\Lambda_{TVPC}$ and not as $(p/\Lambda_{TVPC})^{d-5} \times (1/\Lambda_{TVPC})$ as implied by EFT power counting. As we show below, this loss of power counting prevents one from deriving any information about the $d = 7$ operators from experimental EDM limits. In this respect, our conclusions differ dramatically from those of Refs. [16, 17]. We illustrate this point in the following section.

3 Elementary fermion EDM

The application of EFT for new TVPC interactions to the EDM of an elementary fermion was considered in Ref. [20]. In what follows, we summarize the arguments of that analysis, as they illustrate the general principles of EFT to be used in the remainder of this study. To that end, we first observe that if, as in Scenario B, both new TVPC interactions and PV interactions

(*e.g.*, in the Standard Model) exist at momentum scales $p \gtrsim \Lambda_{TVPC}$, then there exists no reason to assume that the coefficients of the TVPV effective operators in Eq. (4) vanish at tree level. Although we have no detailed knowledge of the dynamics of short-distance TVPC and TCPV interactions, nothing prevents their conspiring to generate non-vanishing low-energy TVPV interactions. In particular, the coefficients of the $d = 5$ electric dipole operators, $C_5^{f\gamma}$ should be non-vanishing at tree-level unless some fortuitous fine-tuning of the short-distance TVPC and TCPV interactions occurs.

The situation here is analogous to the chiral expansion of the octet baryon magnetic moments. In the latter case, the leading order contribution occurs at tree level from the $d = 5$ magnetic moment Lagrangian [22]:

$$\begin{aligned} \mathcal{L}_{M.M} = & \frac{e}{2\Lambda_\chi} \epsilon_{\mu\nu\alpha\beta} v^\alpha \{ b_+ \text{Tr} (\bar{B}_v S^\beta \{ \lambda_3 + \lambda_8/\sqrt{3}, B_v \}) \\ & + b_- \text{Tr} (\bar{B}_v [\lambda_3 + \lambda_8/\sqrt{3}, B_v]) F^{\mu\nu} \} , \end{aligned} \quad (24)$$

where the B_v are the octet baryon fields for states of velocity v^α , S^α is the spin operator, and Λ_χ is the scale of chiral symmetry breaking. The tree level relationship between a baryon magnetic moment and the low-energy constants b_\pm is

$$\mu^a = \left(\frac{m_B}{\Lambda_\chi} \right) b^a \quad , \quad (25)$$

where m_B is the mass of the baryon, “ a ” denotes its SU(3) indices, and b^a is the appropriate combination of the b_\pm . Since the baryon magnetic moments are typically of order unity, the tree-level relation implies that the b_\pm are also of order unity. Alternatively, one may use Eq. (25) to estimate the scale Λ_χ . If the low-energy constants in Eq. (24) are of order unity, the one must have $\Lambda_\chi \sim m_B \sim 1$ GeV. Since the chiral symmetry of pionic interactions implies that $\Lambda_\chi = 4\pi F_\pi \approx 1$ GeV, the tree-level magnetic moment relation produces a self-consistent value for the scale of chiral symmetry breaking when the leading low-energy constants are chosen to be of order one.

In a similar way, one may use the tree-level relation between the EDM and the coefficients of the appropriate $d = 5$ operators to estimate the scale Λ_{TVPC} . This relation is

$$d_f = \frac{C_5^{f\gamma}}{\Lambda_{TVPC}} \quad . \quad (26)$$

We follow a standard convention for parameterizing the strength of new physics interactions and take $C_5^{f\gamma} = 4\pi\kappa^2 e$. Using the present limit for the EDM of the electron $|d_e| < 4 \times 10^{-27}$ e-cm[1, 34], one obtains from Eq. (26) the limit $\Lambda_{TVPC} > 10^{14} \kappa^2$ GeV. Thus, if the new TVPC physics is “strong” ($\kappa^2 \sim 1$), one obtains a tremendously large value for the corresponding mass scale.

For both EFT’s in Eqs. (4, 24), loop corrections involving light, dynamical degrees of freedom modify the tree-level relations in Eqs. (25,26). Single pion loop amplitudes, for example, generate corrections to isovector magnetic moments of $\mathcal{O}(m_\pi/\Lambda_\chi)$ relative to the tree-level contribution. The π loops are quadratically divergent, yet generate a finite contribution to the $d = 5$ magnetic moment operator. Power-counting implies the appearance of one additional mass factor in this finite contribution. When DR is used to regulate the integral, this mass factor becomes m_π , resulting in the m_π/Λ_χ suppression relative to the tree level relation. This scaling behavior of the loop contributions, which follows from the EFT separation of scales, provides for a chiral expansion in powers of p/Λ_χ (where $p < \Lambda_\chi$) which may be reasonably truncated at any order. Similarly, if the EFT of Eq. (4) is well-behaved, one would expect the loop corrections to the relation in Eq. (26) to be suppressed by powers of p/Λ_{TVPC} , where $p < \Lambda_{TVPC}$ is a mass scale associated with the dynamical degrees of freedom in the \mathcal{L}_{NEW} .

For purposes of illustration, we assume that the only dynamical degrees of freedom operative below Λ_{TVPC} are those appearing in the Standard Model. Under Scenario A, additional degrees of freedom – such as the right-handed neutral gauge boson in left-right symmetric theories – would also generate loop contributions. These additional degrees of freedom would be required in order for parity symmetry to be restored for $\mu < \Lambda_{TVPC}$. As noted below, however, the study of only the standard model contributions yields conservative upper bounds on the $d = 7$ TVPC operators. In order to avoid introducing model-dependence associated with parity restoration scenarios, we restrict our attention to these SM effects. In this case, the leading loop corrections are generated by PV Standard Model radiative corrections to the $d = 7$ operators \mathcal{O}_{7a-c} . These corrections have been computed in Ref. [20] for $\mathcal{O}_{7a,c}$ using the diagrams in Figs. 2 and 3. All of the loop amplitudes corresponding to Figs. 2 and 3 are superficially quadratically divergent. The loops are regulated using DR and the poles removed by the corresponding counterterm in the renormalized C_5^f in the $\overline{\text{MS}}$ subtraction scheme. The closed

fermion loop subgraph in Fig. 3a is nominally linearly divergent and corresponds to the Adler-Bell-Jackiw anomaly diagram. In this case, the vector current insertions arise from the γ and Z couplings to the internal fermion, while the axial vector insertion arises from \mathcal{O}_{7a} . Since the EDM operator is linear in the photon momentum q_μ , we follow Ref. [17] and retain only the terms linear in q_μ arising from this sub-graph. Denoting its amplitude $T^{\mu\lambda\alpha}$, we choose the loop momentum routing to satisfy $q^\mu T_{\mu\lambda\alpha} = 0 = k^\lambda T_{\mu\lambda\alpha}$, where q_μ and k_λ are the photon and Z -boson momenta, respectively. The result is the usual anomalous term in $(q+k)^\alpha T_{\mu\lambda\alpha}$. To linear order in q , there exist three structures which satisfy these vector current conservation conditions:

$$A^{\mu\lambda\alpha} = k \cdot q k_\rho \epsilon^{\mu\lambda\rho\alpha} - k^\mu \epsilon^{\sigma\lambda\rho\alpha} q_\sigma k_\rho \quad (27)$$

$$B^{\mu\lambda\alpha} = k^2 q_\nu \epsilon^{\lambda\mu\nu\alpha} - k^\lambda \epsilon^{\rho\mu\nu\alpha} k_\rho q_\nu \quad (28)$$

$$C^{\mu\lambda\alpha} = k^\alpha \epsilon^{\sigma\mu\lambda\rho} q_\sigma k_\rho \quad . \quad (29)$$

The loop integrals for $T^{\mu\lambda\alpha}$ are nominally linearly divergent. As a check on the calculation, we regulate the integrals using two different regulators – Pauli Villars and DR – and obtain identical results in each case. The result is finite:

$$T^{\mu\lambda\alpha} = \frac{1}{8\pi^2} [A^{\mu\lambda\alpha} + 5B^{\mu\lambda\alpha} - 3C^{\mu\lambda\alpha}] \int_0^1 dx \frac{x^2(1-x)}{m_f^2 + x(1-x)k^2} \quad . \quad (30)$$

It is straightforward to verify that when the corresponding term linear in k and quadratic in q , the photon momentum³, is added to the expression in Eq. (30) and the divergence $(q+k)^\alpha T_{\mu\lambda\alpha}$ computed, one obtains the finite, textbook result for $k^2 = q^2 = 0$ [23].

The closed fermion loop of Fig. 3b contains axial vector insertions from \mathcal{O}_{7a} and from the coupling of the Z -boson to the internal fermion. The external fermion line contains the vector current Z -fermion coupling. This sub-graph diverges quadratically and must be renormalized by the appropriate \overline{MS} subtraction before the remaining loop integration is performed. In all cases, the amplitudes are infrared-finite. Consequently, we follow Ref. [17] and neglect the fermion mass dependence entering the loops.

At leading-log order, the results are

$$C_5^f \sim e C_7^{\gamma Z} \left(\frac{M_Z}{\Lambda_{TVP C}} \right)^2 \left(\frac{1}{s_{WCW}} \right) g_A^f \left(\frac{1}{16\pi^2} \right) \ln \frac{M_Z^2}{\mu^2} \quad (31)$$

³Obtained from Eq. (30) by $k \leftrightarrow q$, $\mu \leftrightarrow \lambda$

for the one-loop contribution in Fig. 2, which contains \mathcal{O}_{7c} [24]. The loops in Fig. 3, which contain the four-fermion operator \mathcal{O}_{7a} , yield

$$C_5^f \sim -eC_7^{ff'} \left(\frac{M_Z}{\Lambda_{TVPC}} \right)^2 Q_{f'} g_V^{f'} g_A^f \left(\frac{G_F M_Z^2}{\sqrt{2}} \right) \left(\frac{1}{8\pi^2} \right)^2 \ln \frac{M_Z^2}{\mu^2} \quad (32)$$

for the amplitude of Fig. 3a and

$$C_5^f \sim -eC_7^{ff'} \left(\frac{5}{12} \right) \left(\frac{M_Z}{\Lambda_{TVPC}} \right)^2 Q_f g_V^f g_A^{f'} \left(\frac{G_F M_Z^2}{\sqrt{2}} \right) \left(\frac{1}{8\pi^2} \right)^2 \left(\ln \frac{M_Z^2}{\mu^2} \right)^2 \quad (33)$$

for the amplitude of Fig. 3b. Here, s_W and c_W denote the sine and cosine of the Weinberg angle, respectively, g_V^f and g_A^f denote the vector and axial vector couplings of the Z -boson to fermion f , and Q_f is the corresponding fermion electromagnetic (EM) charge⁴

As expected from general considerations, the results in Eqs. (31-32) display the $(p/\Lambda_{TVPC})^2$ suppression relative to the tree-level relation in Eq. (26), where in this case $p = M_Z$. Thus, if the C_7 have natural size

$$C_{7a} = 4\pi\kappa^2 \quad (34)$$

$$C_{7c} = 4\pi\kappa^2 e g = \frac{4\pi\alpha}{s_W} C_{7a} \quad (35)$$

and if Λ_{TVPC} is determined from the experimental limit on d_e via Eq. (26), then the loop corrections to the tree-level EDM will be suppressed by more than 25 orders of magnitude for new strong interactions ($\kappa^2 \sim 1$). In this case, tree-level dominance of the EDM implies that EDM limits do not provide direct bounds on the $d = 7$ operators appearing in Eq. (4). The situation here is analogous to that of the baryon magnetic moments. Since the latter are generally dominated by the tree-level term, they cannot be used to determine the meson-baryon couplings which enter the one-loop, sub-leading contributions. Instead, the meson-baryon interaction must be determined directly from, *e.g.*, πN scattering and the results used as input into the chiral loop corrections.

The experimental EDM limits could be used to constrain the $d = 7$ TVPC operators directly if – as in Scenario (A) – C_5^f vanishes at tree-level

⁴We have not considered loop effects involving $\mathcal{O}_{7b}^{g\gamma}$. Since they contribute to the EDM at two-loop order, however, we expect them to be no more important than the two-loop contributions involving $\mathcal{O}_{7a}^{ff'}$.

in the EFT. Such a situation could arise under scenarios, such as left-right symmetric gauge theories, in which parity symmetry is restored at some scale well below Λ_{TVPC} . In this case, there would exist no short-distance PV interactions to conspire with the new TVPC physics in generating a tree-level C_5^f . The leading contribution to an elementary fermion EDM would then be given by the results in Eqs. (31-33), with M_Z replaced by, *e.g.*, the scale of parity-restoration (such as the mass of a right-handed gauge boson), and with the appropriate combinations of couplings. Since the low-energy scale (*e.g.*, M_Z) enters quadratically, a conservative upper bound on the C_7/Λ_{TVPC}^3 for this scenario can be obtained by using the Standard Model results given above. The most stringent constraint results from the one-loop amplitude in Eq. (31) applied to the electron EDM. Using the parameterization of Eq. (35), we obtain $\Lambda_{TVPC} \gtrsim 260 \kappa^{2/3}$ TeV. The corresponding two-loop limits are about a factor of five $\sim (16\pi^2)^{1/3}$ weaker. The one-loop constraints from the neutron EDM are also slightly weaker, given the somewhat less stringent experimental limits on d_n [29].

The results of the foregoing analysis have important implications for low-energy direct TVPC searches in light quark systems. These implications are most transparent under Scenario A. In this case, EDM limits constrain the ratio C_7/Λ_{TVPC}^3 via the one- and two-loop results of Eqs. (31-33). As noted in Ref. [18], one expects the ratio α_T to scale as

$$\alpha_T \sim C_7 (p/\Lambda_{TVPC})^3 \quad , \quad (36)$$

where p is a momentum characteristic of low-energy hadronic interactions. Taking $p = 1$ GeV/ c and using the one-loop electron EDM results, one obtains a limit of $\alpha_T \lesssim 10^{-15}$. By comparison, the present direct TVPC search limits are considerably weaker: $\alpha_T \lesssim 10^{-3}$. In short, under the parity-restoration scenario (A), the EDM results provide the most stringent bounds by many orders of magnitude.

For Scenario (B) in which C_5^f does not vanish at tree-level (*e.g.*, PV persists at short distances), the situation is more subtle. In this case the EDM results do not provide direct constraints on the $d = 7$ operators. Nevertheless, one might argue from the EDM limits that the low-energy effects of $d = 7$ operators should be considerably smaller than the present sensitivity of direct TVPC searches. Comparing Eqs. (31-33) to Eq. (36), we infer that the low-energy TVPC effects of the $d = 7$ operators should be suppressed relative to

the corresponding contributions to an EDM by

$$\left(\frac{p}{M_Z}\right)^2 \times (1/\text{loop factors}) \quad . \quad (37)$$

If, in addition, the $d = 7$ loop contributions are already suppressed relative to the tree-level EDM by many orders of magnitude, one would conclude that corresponding effects in low-energy ($p \lesssim 1 \text{ GeV}/c$) TVPC processes would be even smaller – certainly well below the present direct search sensitivity.

Nevertheless, this line of reasoning is not airtight. If $\Lambda_{TVPC} \sim M_Z$, it is conceivable that the tree-level and loop contributions to the EDM can be comparable in magnitude and that, due to possible cancellations, the magnitude of either term can be considerably larger than the EDM limit itself. An analogous situation arises, for example, in the chiral expansion of the isoscalar nucleon magnetic moment. In this case, the leading corrections to the tree-level relation in Eq. (25) arise from kaon loops. Since m_K and Λ_χ do not differ appreciably, the loop corrections are considerably larger than the isoscalar magnetic moment. A similarly large short-distance (tree-level) contribution is needed to cancel the loop effect and obtain the small isoscalar magnetic moment. In this case, the use of the isoscalar magnetic moment, together with power counting and naïve dimensional analysis, to infer either the size of Λ_χ via the tree-level relation Eq. (25) or the size of the one-loop effects would lead to erroneous conclusions. An independent determination of the strength of the loop contribution (*e.g.*, of the kaon-baryon interaction) is needed. Should a similar situation obtain for the EDM, then direct TVPC searches would still be needed to ascertain the scale of the $d = 7$ contributions.

Before concluding our discussion of the elementary fermion EDM, we emphasize the differences between our analysis and that of Ref. [17]. In that work, a calculation of the amplitudes in Fig. 3 was used to try and estimate the size of the short-distance contributions. This estimate was implemented by regulating the two-loop integrals corresponding to Fig. 3 with a form factor of the type

$$F_0(p^2) = (p^2/\Lambda_{TVPC}^2 - 1)^{-1} \quad . \quad (38)$$

The use of this regulator causes the loop integrals to be dominated by contributions from intermediate states having $p \sim \Lambda_{TVPC}$, thereby blurring the separation of scales crucial to the EFT expansion of Eq. (4). Consequently,

the two-loop results of Ref. [17] scale, incorrectly, as $1/\Lambda_{TVPC}$ rather than as $1/\Lambda_{TVPC}^3$. The corresponding implications for low-energy direct TVPC observables are, therefore, erroneous.

More generally, as noted in Ref. [20], the use of a cut-off regulator destroys the power-counting which justifies truncation of the EDM analysis at $d = 7$. This loss of a systematic expansion can be seen by considering the tower of operators

$$\mathcal{O}_{7+2n}^{ff'} = \bar{\psi}_f \overleftrightarrow{D}_\mu \gamma_5 \psi_f (\partial^2)^n \bar{\psi}_{f'} \gamma^\mu \gamma_5 \psi_{f'} \quad , \quad (39)$$

where $n = 0, 1, \dots$. The two-loop calculation of Ref. [17] may be repeated by replacing the insertion of $\mathcal{O}_{7a}^{ff'}$ by each of the operators in Eq. (39). To regulate the divergences, one may, as the calculation of Ref. [17], regulate the integrals with a form factor

$$F_n(p^2) = (p^2/\Lambda_{TVPC}^2 - 1)^{-(1+n)} \quad . \quad (40)$$

The corresponding loop integrals will be the same as those in Ref. [17] but with additional factors of

$$\left(p^2/\Lambda_{TVPC}^2\right)^n \left(p^2/\Lambda_{TVPC}^2 - 1\right)^{-n} \quad (41)$$

$$= \left(p^2/\Lambda_{TVPC}^2 - 1\right)^{-n} \left[\left(p^2/\Lambda_{TVPC}^2 - 1\right)^n + n \left(p^2/\Lambda_{TVPC}^2\right)^{n-1} - \dots \right] \quad (42)$$

$$= 1 + n \left(p^2/\Lambda_{TVPC}^2\right)^{n-1} \left(p^2/\Lambda_{TVPC}^2 - 1\right)^{-n} - \dots \quad (43)$$

appearing in the integrand. The first term ($= 1$) on the RHS of Eq. (43) will yield the same leading-log contribution as obtained in the calculation of Ref. [17]. The remaining terms will generate sub-leading contributions, finite as $\Lambda_{TVPC} \rightarrow \infty$. Thus, at leading-log order, each operator in the tower will generate the *same* contribution, apart from the operator coefficient $C_{7+2n}^{ff'}$, so that the EDM will be proportional to

$$\sum_{n=0}^{\infty} C_{7+2n}^{ff'} \quad . \quad (44)$$

In this case, there exists no reason to isolate the effects of the $d = 7$ operators from those of any other operator in the tower. All contribute with equal weight. It would be erroneous, therefore, to truncate the series at $d = 7$, as was done in Ref. [17], and to argue that the EDM limits constrain the magnitude of only one term in this infinite series.

As this example illustrates, the preservation of the scale separation is crucial to the power counting arguments which justify truncation of the expansion of the EDM at a given order. When DR and $\overline{\text{MS}}$ subtraction is used, for example, the contributions of each operator in the tower (39) will be suppressed by successive powers of $(M_Z/\Lambda_{\text{TVPC}})^2$. To the extent that $M_Z/\Lambda_{\text{TVPC}} < 1$, truncation at $d = 7$ makes for a reasonable approximation. In the remainder of this study, we therefore work with DR and $\overline{\text{MS}}$ subtraction in treating loop effects.

4 Four-quark TVPV Operators

The previous discussion considered the EDM of an elementary fermion. For a composite system such as a neutron, for example, one must also consider many-body contributions involving more than one quark degree of freedom. A generic contribution of this type is shown in Fig. 4. The operators which describe these many-quark effects include the TVPV $d = 6, 7$ operators listed in Eqs. (9, 16). As in the case of the single fermion EDM $\mathcal{O}_5^{f\gamma}$, the $d = 6, 7$ operators may exist at tree-level in the EFT if parity is violated at sufficiently high scales (Scenario B). Similarly, these operators may be renormalized by PV radiative corrections to the $d = 7$ TVPC operators. As with $\mathcal{O}_5^{f\gamma}$, the $\mathcal{O}_{6,7}^{\text{TV}^{\text{PV}}}$ will be dominated by these loop effects if parity symmetry is restored for $\mu < \Lambda_{\text{TVPC}}$ (Scenario A). In what follows, we compute the relevant loop effects.

The leading corrections to the $\mathcal{O}_{6,7}^{\text{TV}^{\text{PV}}}$ are generated by the set of graphs illustrated in Fig. 5, where the operator inserted is $\mathcal{O}_{7a}^{ff'}$. The diagrams of Fig. 5a were considered previously in the study of Ref. [16]. The diagrams for Fig. 5b, which are required by electromagnetic (EM) gauge invariance, were not included in that analysis. The inclusion of these graphs is needed in order to obtain the pieces of the $d = 7$ TVPV operators containing the photon field. As we discuss in Section 6, the contributions from these γ -insertion diagrams to the neutron EDM are numerically as large as the contributions arising from the graphs of Fig. 5a. The reason for this situation is relatively straightforward. The diagrams in Fig. 5a yield the pieces of the $d = 7$ operators containing a derivative, as well as contributions to the $d = 6$ operators

proportional to one power of quark mass⁵. When the derivative operator acts on quarks inside the hadron, the result is of order $\lesssim \Lambda_{QCD}$. The resulting contribution to the neutron EDM, as in Fig. 4a for example, will therefore go as $\Lambda_{QCD}/\Delta M$, where ΔM is the mass difference between the neutron and one of its excited states (*e.g.*, an unbound $\pi^- p$ pair). The γ -insertion diagrams of Fig. 4b do not produce such derivative operators, and their corresponding neutron EDM contributions contain no $\Lambda_{QCD}/\Delta M$ factors. To the extent that $\Lambda_{QCD}/\Delta M$ is of order one, the magnitude of the two sets of contributions should be comparable.

The amplitudes, \mathcal{M}_5 , of Fig. 5 are logarithmically divergent. As before, we regulate the loops using DR and define the finite results using $\overline{\text{MS}}$ subtraction. At leading-log order, the sum of all twenty six diagrams yields the following linear combination of the $\mathcal{O}_{6,7}^{TVPV}$:

$$\begin{aligned} \mathcal{M}_5 = & \frac{C_{7a}^{ff'}}{\Lambda_{TVP}^3} \frac{\alpha}{32\pi s_W^2 c_W^2} \log\left(\frac{\mu^2}{M_Z^2}\right) \left\{ 6m_{f'} g_V^f g_A^{f'} \mathcal{O}_{6a}^{ff'} \right. \\ & + g_V^f \frac{(g_A^f + g_A^{f'})}{2} [3\mathcal{O}_{7e}^{ff'} + \mathcal{O}_{7g}^{f'f}] \\ & + m_{f'} g_A^{f'} g_V^f \mathcal{O}_{6c}^{f'f} + (g_A^{f'} g_V^f - 2g_A^{f'} g_V^{f'} - 2g_A^f g_V^{f'}) \mathcal{O}_{7f}^{f'f} \\ & \left. - \frac{3}{2} g_A^f g_V^{f'} \mathcal{O}_{7h}^{f'f} + \frac{1}{2} g_A^f g_V^{f'} \mathcal{O}_{7j}^{f'f} \right\} . \end{aligned} \quad (45)$$

The expression in Eq. (45) is obtained by keeping the external fermion lines off shell. Doing so allows us to identify uniquely the contributions of the $d = 7$ TVPV derivative operators and verify the gauge invariance of the overall result.

In order to compare our result with the calculation of Ref. [16], we use the equations of motion and let the quarks go on shell and convert to momentum space. We obtain

$$\begin{aligned} \mathcal{M}_5 = & \frac{C_{7a}^{ff'}}{\Lambda_{TVP}^3} \frac{\alpha}{32\pi s_W^2 c_W^2} \log\left(\frac{\mu^2}{M_Z^2}\right) \left[6im_{f'} g_V^f g_A^{f'} \bar{U}_f \gamma_5 U_f \bar{U}_{f'} U_{f'} \right. \\ & \left. - 2im_{f'} g_V^f (g_A^f + g_A^{f'}) \bar{U}_f U_f \bar{U}_{f'} \gamma_5 U_{f'} \right] \end{aligned}$$

⁵Since the $d = 6$ operators do not preserve chirality, they cannot be induced dynamically by massless quarks.

$$\begin{aligned}
& +im_{f'}g_A^{f'}g_V^f\bar{U}_f\gamma_5\sigma^{\mu\nu}U_f\bar{U}_{f'}\sigma_{\mu\nu}U_{f'} \\
& +i\left(2g_A^{f'}g_V^{f'}-g_A^{f'}g_V^f+\frac{7}{2}g_A^fg_V^{f'}\right)\bar{U}_f\gamma_5(p'_{f'}+p_f)^\mu U_f\bar{U}_{f'}\gamma_\mu U_{f'} \\
& +\frac{1}{2}g_A^fg_V^{f'}\bar{U}_f\sigma^{\mu\nu}U_f\bar{U}_{f'}(p'_{f'}+p_{f'})_\nu\gamma_\mu\gamma_5U_{f'}\quad , \quad (46)
\end{aligned}$$

where $U_f \equiv U(p_f)$ and $\bar{U}_f \equiv \bar{U}(p'_f)$ are the spinors for incoming and outgoing fermions f , respectively.

The first three of the terms on the RHS of Eq. (46) are identical to those appearing in [16]. Our coefficient of the fourth term, however, differs from the corresponding expression in [16], and the fifth term does not appear in that work at all. We trace part of the difference on the fourth term to diagrams in Fig. 5a where the Z^0 boson connects to initial and final quarks of the same species. It is unclear from the discussion of Ref. [16] whether those authors included this class of diagrams. Given that our sum of the amplitudes for Figs. 5a and 5b satisfies a gauge invariance self-consistency check, we are confident in our result.

5 Hadronic Matrix Elements

The operators obtained in the previous sections can be used to compute contributions to the EDM of the neutron and of neutral atoms. Doing so requires that one calculate various hadronic matrix elements of two- and four-quark operators. A first principles treatment of these matrix elements in QCD goes beyond the scope of the present study. Moreover, since we seek only to derive order of magnitude constraints on new TVPC interactions and not to obtain definitive numerical results, it suffices to draw upon various approximation methods. To that end, we turn to the quark model [25], factorization, and chiral symmetry.

Below, we estimate a number of different matrix elements relevant to the neutron EDM and couplings \bar{g}_ρ and $\bar{g}_\pi^{(a)}$:

1. The contribution to d_n from quark EDMs (Fig. 6)
2. The relationship between \bar{g}_ρ and $d = 7$ TVPC operators (Fig. 7a) and the relationship between \bar{g}_ρ and d_n (Fig. 7b).

3. The contribution to d_n from the four-quark/photon TVPV operators appearing in Eq. (45) (Fig. 4b).
4. The contribution to the $\bar{g}_\pi^{(a)}$ from the purely hadronic terms in Eq. (45) (Fig.8a) and the relationship between the $\bar{g}_\pi^{(a)}$ and d_n (Fig. 8b).
5. The tree-level contribution from $\mathcal{O}_{7c}^{Z\gamma}$ (Fig. 9).

A. Two-quark TVPV Operators

Relating the EDM of a constituent quark to that of the neutron using the quark model is a straightforward exercise. As shown in Ref. [20], this relationship is given by

$$d_n = \frac{1}{\Lambda_{TVPC}} \left[\frac{4}{3} C_5^d - \frac{1}{3} C_5^u \right] \int d^3x \left(u^2 + \frac{1}{3} \ell^2 \right) , \quad (47)$$

where u and ℓ are the upper and lower component quark model radial wave functions, respectively. The integral in Eq. (47) can be estimated using the wave function normalization condition

$$\int d^3x \left(u^2 + \ell^2 \right) = 1 \quad (48)$$

and expression for the axial vector charge

$$g_A = \frac{5}{3} \int d^3x \left(u^2 - \frac{1}{3} \ell^2 \right) , \quad (49)$$

where $g_A \approx 1.26$. From Eqs. (48-49) one obtains

$$\int d^3x \left(u^2 + \frac{1}{3} \ell^2 \right) = \frac{1}{4} \left(2 + \frac{6}{5} g_A \right) \approx 0.88 \quad . \quad (50)$$

B. Four-Quark TVPC Operators

Deriving the relationship between the effective hadronic coupling \bar{g}_ρ and the four-quark $d = 7$ TVPC operators (Fig. 7a) requires more thought than in the case of evaluating two-quark matrix elements. For simplicity, we focus on the four-quark operator $\mathcal{O}_{7a}^{ff'}$. We make a simple estimate using factorization. Doing so requires use of the Fierz transformed version of this

operator, since the interaction in Eq. (2) involves only ρ^\pm . The Fierzed form of the operator is

$$\begin{aligned}
\mathcal{O}_{7a}^{ff'} = & -\left(\frac{3}{4}\bar{\psi}_f\overleftarrow{\partial}_\nu\psi_{f'}\bar{\psi}_{f'}\gamma_\nu\psi_f + \frac{3}{4}\bar{\psi}_f\psi_{f'}\bar{\psi}_{f'}\gamma_\nu\overrightarrow{\partial}_\nu\psi_f\right. \\
& +\frac{3}{4}\bar{\psi}_f\gamma_\nu\overleftarrow{\partial}_\nu\psi_{f'}\bar{\psi}_{f'}\psi_f + \frac{3}{4}\bar{\psi}_f\gamma_\nu\psi_{f'}\bar{\psi}_{f'}\overrightarrow{\partial}_\nu\psi_f \\
& +\frac{i}{4}\bar{\psi}_f\overleftarrow{\partial}_\nu\gamma_\mu\psi_{f'}\bar{\psi}_{f'}\sigma_{\mu\nu}\psi_f + \frac{i}{4}\bar{\psi}_f\gamma_\mu\psi_{f'}\bar{\psi}_{f'}\sigma_{\mu\nu}\overrightarrow{\partial}_\nu\psi_f \\
& -\frac{i}{4}\bar{\psi}_f\overleftarrow{\partial}_\nu\sigma_{\mu\nu}\psi_{f'}\bar{\psi}_{f'}\gamma_\mu\psi_f - \frac{i}{4}\bar{\psi}_f\sigma_{\mu\nu}\psi_{f'}\bar{\psi}_{f'}\gamma_\mu\overrightarrow{\partial}_\nu\psi_f \\
& +\frac{3}{4}\bar{\psi}_f\overleftarrow{\partial}_\nu\gamma_5\psi_{f'}\bar{\psi}_{f'}\gamma_\nu\gamma_5\psi_f + \frac{3}{4}\bar{\psi}_f\gamma_5\psi_{f'}\bar{\psi}_{f'}\gamma_\nu\gamma_5\overrightarrow{\partial}_\nu\psi_f \\
& -\frac{3}{4}\bar{\psi}_f\overleftarrow{\partial}_\nu\gamma_\nu\gamma_5\psi_{f'}\bar{\psi}_{f'}\gamma_5\psi_f - \frac{3}{4}\bar{\psi}_f\gamma_\nu\gamma_5\psi_{f'}\bar{\psi}_{f'}\gamma_\nu\gamma_5\overrightarrow{\partial}_\nu\psi_f \\
& +\frac{i}{4}\bar{\psi}_f\overleftarrow{\partial}_\nu\gamma_5\sigma_{\mu\nu}\psi_{f'}\bar{\psi}_{f'}\gamma_5\gamma_\mu\psi_f + \frac{i}{4}\bar{\psi}_f\gamma_5\sigma_{\mu\nu}\psi_{f'}\bar{\psi}_{f'}\gamma_5\gamma_\mu\overrightarrow{\partial}_\nu\psi_f \\
& \left. +\frac{i}{4}\bar{\psi}_f\overleftarrow{\partial}_\nu\gamma_5\gamma_\mu\psi_{f'}\bar{\psi}_{f'}\gamma_5\sigma_{\mu\nu}\psi_f + \frac{i}{4}\bar{\psi}_f\gamma_5\gamma_\mu\psi_{f'}\bar{\psi}_{f'}\gamma_5\sigma_{\mu\nu}\overrightarrow{\partial}_\nu\psi_f\right)
\end{aligned} \tag{51}$$

In the factorization approximation, one makes the replacement

$$\langle N'|\bar{q}_i^{-1}O_1q_j^2\bar{q}_j^2O_2q_i^1|N\rho\rangle \rightarrow \langle 0|\bar{q}_i^{-1}O_1q_j^2|\rho\rangle\langle N'|\bar{q}_j^2O_2q_i^1|N\rangle \quad , \tag{52}$$

where N and N' denote nucleons, q_i^a is the field for a quark of flavor a and color i , and $\bar{q}_i^{-1}O_1q_j^2\bar{q}_j^2O_2q_i^1$ denotes any of the products of quark bilinears appearing in Eq. (51). Note that since hadrons are color singlets, one has

$$\langle 0|\bar{q}_i^{-1}O_1q_j^2|\rho\rangle = \frac{1}{3}\delta_{ij}\langle 0|\bar{q}_k^{-1}O_1q_k^2|\rho\rangle \tag{53}$$

$$\langle N'|\bar{q}_j^2O_2q_i^1|N\rangle = \frac{1}{3}\delta_{ij}\langle N'|\bar{q}_m^2O_2q_m^1|N\rangle \quad , \tag{54}$$

where repeated indices are summed over. Hence, each factorization contribution contains a factor of

$$\frac{1}{3}\delta_{ij} \times \frac{1}{3}\delta_{ji} = \frac{1}{3} \quad . \tag{55}$$

Since any pieces of the interaction above which involve the γ_5 will not give rise to a ρ meson-vacuum matrix element, we are concerned with only the

first eight terms of the Fierzed interaction. We may also reduce the number of terms to be evaluated using the equations of motion. Of the resulting operators, we keep only those containing no powers of the quark mass, since the latter generate significant suppression factors. In the case where f represents an up quark and f' represents a down quark, the remaining structures are

$$\frac{1}{2}\bar{u}\overleftarrow{\partial}_\nu d\bar{d}\gamma^\nu u + \frac{1}{2}\bar{u}\gamma^\nu d\bar{d}\overrightarrow{\partial}_\nu u - \frac{i}{4}\bar{u}\overleftarrow{\partial}_\nu\gamma_\mu d\bar{d}\sigma^{\mu\nu}u + \frac{i}{4}\bar{u}\sigma^{\mu\nu}d\bar{d}\gamma_\mu\overrightarrow{\partial}_\nu u. \quad (56)$$

In the factorization approximation, the matrix elements required are

$$\begin{aligned} &\langle 0|\bar{u}\overleftarrow{\partial}_\mu d|\rho^-\rangle\langle n|\bar{d}\gamma^\mu u|p\rangle, \\ &\langle 0|\bar{u}\gamma^\mu d|\rho^-\rangle\langle n|\bar{d}\overrightarrow{\partial}_\mu u|p\rangle \\ &\langle 0|\bar{u}\overleftarrow{\partial}_\nu\gamma_\mu d|\rho^-\rangle\langle n|\bar{d}\sigma^{\mu\nu}u|p\rangle, \\ &\langle 0|\bar{u}\sigma^{\mu\nu}d|\rho^-\rangle\langle n|\bar{d}\gamma_\mu\overrightarrow{\partial}_\nu u|p\rangle, \end{aligned} \quad (57)$$

plus the corresponding matrix elements for $\rho^+n \rightarrow p$ (note that in Eq. (57) the color indices have been suppressed for simplicity). A detailed evaluation of these matrix elements appears in Appendix A. The resulting TVPC ρNN Lagrangian is

$$\mathcal{L} = i\sqrt{2}\frac{C_{7a}^{ud}}{\Lambda_{TVPC}^3}\frac{m_\rho^2}{f_\rho}\frac{1}{6}\bar{N}\left[\left(\frac{1.05}{R_\rho} - \frac{1.293}{R_n}\right)\gamma^\mu\right. \quad (58)$$

$$\left.+i\left(0.176\frac{R_n}{R_\rho} - 0.122\right)q_\nu\sigma^{\mu\nu}\right](\tau^-\rho_\mu^+ - \tau^+\rho_\mu^-)N \quad (59)$$

It is customary to write the standard rho-nucleon Lagrangian and the TVPC rho-nucleon Lagrangian in the respective forms (see, *e.g.* Eq. (2),

$$\mathcal{L} = \sqrt{2}f_\rho\bar{N}(\gamma^\mu + i\frac{\kappa_V}{2m_n}\sigma^{\mu\lambda}q_\lambda)(\tau^-\rho_\mu^+ + \tau^+\rho_\mu^-)N \quad (60)$$

$$\mathcal{L}_{TVPC} = \sqrt{2}\bar{g}_\rho f_\rho\frac{\kappa_V}{2m_n}\bar{N}\sigma^{\mu\lambda}q_\lambda(\tau^-\rho_\mu^+ - \tau^+\rho_\mu^-)N \quad (61)$$

where κ_V is the anomalous isovector magnetic moment, m_n is the mass of the nucleon and f_ρ is the ρNN coupling constant. By redefining the phase of the rho meson, we can eliminate the Dirac structure γ^μ in Eq. (58). We

begin by writing Eqs. (58) and (60) together as

$$\begin{aligned} \mathcal{L}_{\rho NN} = & \sqrt{2}f_\rho \bar{N} \left[\gamma^\mu \left(1 + \frac{iA}{f_\rho}\right) + i\frac{\kappa_V}{2m_n} \left(1 + iB\frac{2m_n}{f_\rho \kappa}\right) \sigma^{\mu\lambda} q_\lambda \right] \tau^- \rho_\mu^+ N \\ & + \sqrt{2}f_\rho \bar{N} \left[\gamma^\mu \left(1 - \frac{iA}{f_\rho}\right) + i\frac{\kappa_V}{2m_n} \left(1 - iB\frac{2m_n}{f_\rho \kappa}\right) \sigma^{\mu\lambda} q_\lambda \right] \tau^+ \rho_\mu^- N \end{aligned} \quad (62)$$

where

$$A = \frac{1}{6} \frac{C_{7a}^{ud}}{\Lambda_{TVP}^3} \frac{m_\rho^2}{f_\rho} \left[\frac{1.05}{R_\rho} - \frac{1.293}{R_n} \right] \quad (63)$$

$$B = \frac{1}{6} \frac{C_{7a}^{ud}}{\Lambda_{TVP}^3} \frac{m_\rho^2}{f_\rho} \left(0.176 \frac{R_n}{R_\rho} - 0.122 \right) \quad (64)$$

We then observe that since $1+iA/f_\rho \approx \exp(iA/f_\rho)$ and $1+iB2m_n/(f_\rho \kappa_V) \approx \exp[iB/(f_\rho \kappa_V)]$, the phases of the rho mesons can be redefined as, $\rho_\mu^+ \rightarrow \tilde{\rho}_\mu^+ \exp(-iA/f_\rho)$ and $\rho_\mu^- \rightarrow \tilde{\rho}_\mu^- \exp(iA/f_\rho)$. This allows us to rewrite the total Lagrangian as

$$\begin{aligned} \mathcal{L} \approx & \sqrt{2}f_\rho \bar{N} \left[\gamma^\mu + i\frac{\kappa_V}{2m_n} \sigma^{\mu\nu} q_\nu \right] (\tau^- \tilde{\rho}_\mu^+ + \tau^+ \tilde{\rho}_\mu^-) N \\ & - \sqrt{2}f_\rho \bar{N} \left(\frac{B2m_n}{f_\rho \kappa_V} - \frac{A}{f_\rho} \right) \frac{\kappa_V}{2m_n} \sigma^{\mu\nu} q_\nu (\tau^- \tilde{\rho}_\mu^+ - \tau^+ \tilde{\rho}_\mu^-) N \end{aligned} \quad (65)$$

The quantity \bar{g}_ρ is then

$$\bar{g}_\rho = \frac{C_{7a}^{ud}}{3} \left(\frac{m_n m_\rho^2}{\Lambda_{TVP}^3} \right) \frac{1}{f_\rho^2 \kappa_V} \left[\left(\frac{1.05}{R_\rho} - \frac{1.293}{R_n} \right) \frac{\kappa_V}{2m_N} - \left(0.176 \frac{R_n}{R_\rho} - 0.122 \right) \right] \quad (66)$$

where

$$\left(\frac{1.05}{R_\rho} - \frac{1.293}{R_n} \right) \frac{\kappa_V}{2m_N} - \left(0.176 \frac{R_n}{R_\rho} - 0.122 \right) \sim -0.023 \quad . \quad (67)$$

As calculated in Ref. [27], \bar{g}_ρ may contribute to the neutron EDM via the loop diagrams of Fig. 7(b) as well as to the atomic EDM via process like those shown in Figs. 1(a,b). The d_n calculation of Ref. [27] included the introduction of form factors at the hadronic vertices in order to render the loop integrals finite. The result is

$$\frac{d_n}{e} = \frac{h_{\pi NN} g_{\rho\pi\gamma} f_\rho \bar{g}_\rho \kappa_V}{16\sqrt{2}\pi^2 m_\rho} \tilde{F}(m_\pi, m_\rho, m_N, \Lambda) \quad (68)$$

where $g_{\rho\pi\gamma} = 0.4$ and the PV pion-nucleon coupling $h_{\pi NN}$ is constrained by the PV γ -decay of ^{18}F to lie in the range: $h_{\pi NN} = (0.73 \pm 2.3)g_\pi$, where $g_\pi = 3.8 \times 10^{-8}$ characterizes the strength of the charged current $\Delta S = 0$ hadronic interaction. The function \tilde{F} depends on the masses appearing in the loop integral as well as the form factor cut-off parameter, Λ .

We note that the use of Eq. (68) and the experimental limits on d_n to derive bounds on TVPC interactions entails several ambiguities. First, the value of $h_{\pi NN}$ measured in nuclei such as ^{18}F may differ from the value appropriate to the single nucleon or few-nucleon systems. Many-body nuclear effects may renormalize the long range PV NN interaction in such a way as to shift the value of the effective PV πNN coupling from the value appropriate for Eq. (68). This ambiguity may be resolved by future experiments, such as the measurement of the $\vec{n} + p \rightarrow d + \gamma$ asymmetry planned at LANSCE[28].

Second, the use of a form factor to render the loop integral finite can introduce considerable ambiguity. The form factor chosen in Ref. [27] was taken from the Bonn potential, with $\Lambda = 1.4$ GeV. One may just as well have chosen a cut-off given by the inverse size of the hadron. The variations due to this spread of choices can be significant [22]. Moreover, as argued in Section 3, the use of cut-off regulators can render one's effective theory devoid of any systematic power counting, leaving it poorly defined. For these reasons, we will not use Eq. (68) to derive limits on the $d = 7$ TVPC operators.

C. Four-Quark TVPV Operators

We consider the relationship between the $d = 6$ and $d = 7$ TVPV operators and the neutron EDM. We specify here to Scenario (A), in which case the TVPV operators arise entirely from PV radiative corrections to the TVPC operators, as in Fig. 5. First, we estimate the contribution from the pieces of the $d = 7$ operators containing the photon field. These contributions can be understood diagrammatically as shown in Fig 4(b). Starting from expression in Eq. (45), we see that the TVPV γ -four-quark interaction can be written as

$$\begin{aligned} \mathcal{L}_{eff}^{TVPV,EM} &= e\mathcal{J}_\lambda^{eff} A^\lambda \\ &= e\frac{C_{7a}^{ff'}}{\Lambda_{TVPC}^3} \frac{\alpha}{32\pi s_W^2 c_W^2} \log\left(\frac{\mu^2}{M_Z^2}\right) \left[\right. \\ &\quad \left. + [g_V^{f'} g_A^f - g_V^f (g_A^{f'} + g_A^f)] \bar{\psi}_f \sigma_{\lambda\mu} \psi_f \bar{\psi}_{f'} \gamma_5 \gamma_\mu \psi_{f'} \right] \end{aligned}$$

$$+g_V^{f'} g_A^f 3i\bar{\psi}_f \gamma_5 \psi_f \bar{\psi}_{f'} \gamma_\lambda \psi_{f'} \Big] A^\lambda \quad . \quad (69)$$

For simplicity, we consider the case where f is an up quark and f' denotes a down quark. As in our estimate of \bar{g}_ρ , we can find neutron matrix elements using the quark model. We identify the appropriate quark model expression for the electric dipole moment,

$$i\langle n\lambda' | \int d^3x_3 \mathcal{J}_0^{eff} | n\lambda \rangle_{QM} = \frac{d_n}{e} \int d^3p \bar{u}(p, \lambda') \sigma_{03} \gamma_5 u(p, \lambda) |\phi(p)|^2 \quad . \quad (70)$$

Here, $|n\lambda\rangle$ is a neutron in the $S_z = \lambda$ state, the $\phi(p)$ are used in the wave packet description of the momentum eigenstates as discussed in Appendix A, and the $u(p, \lambda)$ are the neutron spinors. Choosing $\lambda = \lambda' = 1/2$ we have

$$\langle n1/2 | \int d^3x_3 \mathcal{J}_0^{eff} | n1/2 \rangle_{QM} = \frac{d_n}{e} \quad . \quad (71)$$

We evaluate the two matrix elements needed and find

$$\langle n | \bar{u} \gamma_5 u \bar{d} \gamma_0 d | n \rangle = i \frac{8 \cdot 0.8623}{9 \cdot 4\pi R_n^2} \quad (72)$$

$$\langle n | \bar{u} \sigma^{0\mu} u \bar{d} \gamma_5 \gamma_\mu d | n \rangle = \frac{4 \cdot 0.8623}{9 \cdot 4\pi R_n^2} \quad . \quad (73)$$

Using these matrix elements, we obtain the following expression for the neutron EDM:

$$\frac{d_n}{e} = -\frac{C_{7a}^{ud}}{\Lambda_{TVPV}} \left(\frac{1}{\Lambda_{TVPV}^2 R_n^2} \right) \frac{\alpha}{32\pi s_W^2 c_W^2} \log \left(\frac{\mu^2}{M_Z^2} \right) \quad (74)$$

$$\times \frac{0.4}{4\pi} [g_V^d (g_A^u + g_A^d) + 5.5 g_A^d g_V^u] \quad (75)$$

Since $g_A^u + g_A^d \approx 0$ in the Standard Model⁶, this contribution to the neutron electric dipole moment is approximately proportional to $g_A^d g_V^u$.

The second way TVPV operators contribute to d_n is by mixing states of opposite parity into the neutron ground state (Fig. 4a). The lightest state which may contribute is the $N\pi$ S-wave. In the chiral limit, its contribution is

⁶The sum is exactly zero at tree-level.

dominated by the loop diagrams of Fig. 8(b). The TVPV $NN\pi$ couplings are just the $\bar{g}_\pi^{(I)'}$, generated from the TVPV quark operators as in Fig. 8(a). The $\bar{g}_\pi^{(I)'}$ also contribute to the atomic EDM via the meson-exchange interaction of Fig. 1(c). In what follows, we relate the $\bar{g}_\pi^{(I)'}$ to the purely hadronic parts of the operators in Eq. (45).

Following Ref. [16], we carry out the calculation in the factorization approximation while using the on-shell form of the TVPV operators given in Eq. (46). First, we consider the TVPV $NN\pi^0$ coupling. The only Dirac structures which give rise to pion-vacuum matrix elements are γ_5 , and $\gamma_5\gamma^\mu$. Therefore the structure in the third line does not contribute. The last two structures in Eq. (46) do not contribute in the factorization approximation. This conclusion follows from symmetry arguments, $p_\pi^\mu p_\pi^\nu \sigma_{\mu\nu} = 0$, and the equations of motion $p_\pi^\mu \bar{N} \gamma_\mu N = 0$. For the remaining structures the PCAC relation

$$\frac{1}{2} \langle 0 | \bar{u} \gamma^\mu \gamma_5 u - \bar{d} \gamma^\mu \gamma_5 d | \pi^0 \rangle = i f_\pi p^\mu \exp(-ip \cdot x). \quad (76)$$

Taking the divergence of Eq. (76) and using the consequences of isospin symmetry

$$\langle 0 | \bar{u} \gamma_5 u + \bar{d} \gamma_5 d | \pi^0 \rangle = 0 \quad (77)$$

yields the following two matrix elements needed in the calculation:

$$\langle 0 | \bar{u} \gamma_5 u | \pi^0 \rangle = -i \frac{m_\pi^2 f_\pi}{m_u + m_d} \exp(-ip \cdot x) \quad (78)$$

$$\langle 0 | \bar{d} \gamma_5 d | \pi^0 \rangle = i \frac{m_\pi^2 f_\pi}{m_u + m_d} \exp(-ip \cdot x) \quad (79)$$

In addition, we require the nucleon matrix elements of the light quark scalar densities. From the quark model and πN sigma term, one obtains

$$\langle n | \bar{u} u | n \rangle = \langle p | \bar{d} d | p \rangle \approx 5 \quad (80)$$

$$\langle n | \bar{d} d | n \rangle = \langle p | \bar{u} u | p \rangle \approx 6 \quad (81)$$

Using these results, we obtain for the TVPV neutral pion nucleon couplings $A\bar{n}\pi^0 n$ and $B\bar{p}\pi^0 p$, the strength of the couplings are:

$$A = \frac{C_{7a}^{ud}}{3} \frac{f_\pi m_\pi^2}{\Lambda_{TVPC}^3} \frac{\alpha}{32\pi s_W^2 c_W^2} \log\left(\frac{\mu^2}{M_Z^2}\right) \frac{m_d}{m_u + m_d} 36 \left[g_V^u g_A^d + \frac{10}{36} g_V^u (g_A^u + g_A^d) \right] \quad (82)$$

$$B = \frac{C_{7a}^{ud}}{3} \frac{f_\pi m_\pi^2}{\Lambda_{TVP}^3} \frac{\alpha}{32\pi s_W^2 c_W^2} \log\left(\frac{\mu^2}{M_Z^2}\right) \frac{m_d}{m_u + m_d} 30 \left[g_V^u g_A^d + \frac{2}{5} g_V^u (g_A^u + g_A^d) \right] \quad (83)$$

Here again, since $g_A^u + g_A^d = 0$ at tree level in the Standard Model, the terms proportional to $g_V^u g_A^d$ make the largest contribution.

In order to determine the couplings of the charged pion with the nucleon, we Fierz transform Eq. (46). The result is listed in Appendix B. As discussed in Appndix B, we estimate the strength of the $C\bar{p}\pi^-n$ coupling using the first two terms in the Fierz transformed expression. The remaining terms do not contribute in the factorization approximation. In this case, we require the following matrix elements:

$$\langle 0|\bar{u}\gamma_5 d|\pi^- \rangle = \langle \pi^-|\bar{d}\gamma_5 u|0 \rangle = i\sqrt{2} \frac{f_\pi m_\pi^2}{m_u + m_d}; \quad (84)$$

$$\langle n|\bar{d}u|p \rangle = \langle p|\bar{u}d|n \rangle \approx 1. \quad (85)$$

The coefficient can then be written as,

$$C = -\sqrt{2} \frac{C_{7a}^{ud}}{3} \left(\frac{f_\pi m_\pi^2}{\Lambda_{TVP}^3} \right) \frac{\alpha}{32\pi s_W^2 c_W^2} \log\left(\frac{\mu^2}{M_Z^2}\right) \times \frac{m_d}{m_u + m_d} \left(4g_V^u g_A^d - \frac{1}{2} g_V^u g_A^u + \frac{3}{4} g_V^d g_A^u \right) \quad (86)$$

The last piece $3g_V^u g_A^d/4$ comes from applying equations of motion to the derivative terms, as discussed in Appendix B.

Expressed in terms of A, B and C, the PVTV pion-nucleon couplings from Eq. (3) are

$$\bar{g}_\pi^{(0)'} = (B - A)/6 + \sqrt{2}C/3 \quad (87)$$

$$\bar{g}_\pi^{(1)'} = (A + B)/2 \quad (88)$$

$$\bar{g}_\pi^{(2)'} = (B - A)/6 - \frac{C}{3\sqrt{2}} \quad (89)$$

In the chiral expansion of the EDM, the dominant contribution to d_n from the TVPV πNN interaction arises from the loops in Fig. 8(b), where the intermediate state contains a $p\pi^-$. In this case, only the constant C contributes. The loop calculation, first performed in Ref. [30], yields

$$\frac{d_n}{e} = \frac{C}{\sqrt{2}} \frac{g_{\pi NN}}{4\pi^2 m_N} \log \frac{m_N}{m_\pi} . \quad (90)$$

Written explicitly in terms of the TVPC scale, Λ_{TVPC} , the neutron electric dipole moment takes the form,

$$\frac{d_n}{e} = \left(\frac{C_{7a}^{ud}}{\Lambda_{TVPC}} \right) \left(\frac{m_\pi^2}{\Lambda_{TVPC}^2} \right) \left(\frac{f_\pi}{m_N} \right) \frac{1}{3} \frac{\alpha}{32\pi s_W^2 c_W^2} \frac{g_{\pi NN}}{4\pi^2} \log \frac{m_\pi}{m_N} \log \left(\frac{\mu^2}{M_Z^2} \right) \frac{m_d}{m_u + m_d} \left(4g_V^u g_A^d - \frac{1}{2} g_V^u g_A^u + \frac{3}{4} g_V^d g_A^u \right) \quad , \quad (91)$$

where we have kept only the leading, non-analytic loop contribution proportional to $\log(m_\pi/m_N)$ and where $g_{\pi NN}$ is the strong πNN coupling. We note that an evaluation of the analytic contributions has been performed using sidewise dispersion relations in Ref. [31]. In addition, loop contributions involving the $n\pi^0$ intermediate state have been considered in Refs. [32, 33].

D. Tree-level contributions

There exists one way in which the $d = 7$ TVPC operators may contribute to d_n without the consideration of loop effects. As shown in Fig. 9, the operator $\mathcal{O}_{7c}^{Z\gamma}$ generates a tree-level contribution when the Z^0 is exchanged and couples to the second quark's axial vector current. Naïvely, one might expect this contribution to compete with the one-loop quark EDM generated by $\mathcal{O}_{7c}^{Z\gamma}$ in Fig. 2. The calculation of the process in Fig. 9 is tedious but straightforward. Using the quark model, we obtain

$$\begin{aligned} \frac{d_n}{e} &= -\frac{1}{\Lambda_{TVPC}} \left[\frac{C_{7c}^{Z\gamma} g_A^d}{2s_W} \right] \left(\frac{M_Z}{\Lambda_{TVPC}} \right)^2 \left[\frac{0.34}{M_Z^3 M_W R_n^4} \right] \\ &\times \int_0^{2.04} x^2 dx \left[j_0(x)^2 j_0'(x) j_1(x) - j_0(x) j_1(x)^2 j_1'(x) - j_0(x) j_1(x)^3 / x \right] \\ &\times \sum_{m, m', \alpha, \dots} \sigma_{mm}^3 \langle n1/2 | u^\dagger(m', \alpha') u(m', \alpha) d^\dagger(m, \beta') d(m, \beta) | n1/2 \rangle \quad , \end{aligned} \quad (92)$$

where the sum runs over all spin (m, m') and color (α, β, \dots) indices. Evaluating the integrals and quark model contractions yields

$$\frac{d_n}{e} = \frac{1}{\Lambda_{TVPC}} \left[\frac{C_7^{Z\gamma} g_A^d}{2s_W} \right] \left(\frac{M_Z}{\Lambda_{TVPC}} \right)^2 \left[\frac{0.162}{M_Z^3 M_W R_n^4} \right] \quad . \quad (93)$$

Comparing the result in Eq. (93) with one-loop amplitude in Eq. (31), we observe that the tree-level contribution contains the suppression factor

$$\frac{0.162}{M_Z^3 M_W R_n^4} \approx 8.64 \times 10^{-12} \quad . \quad (94)$$

The difference results from the contributions of high-momentum ($p \sim M_Z$) intermediate states in the loops of Fig. 2. The tree-level process, in contrast, is dominated by states with momenta $p \lesssim \Lambda_{QCD} \sim 0.002M_Z$. Since the TVPC operator has dimension seven, and since the momentum transferred through Z^0 -boson propagator in Fig. 9 is $\lesssim \Lambda_{QCD}$, one would expect a suppression factor of $(\Lambda_{QCD}/M_Z)^4 \sim 10^{-11}$ for the process of Fig. 9.

6 Experimental Constraints

The foregoing analysis allows us to make a quantitative connection between various observables and effective coupling constants on the one side and the EFT of TVPC interactions of quarks and gauge bosons on the other. In this section, we use those relationships to derive bounds on the TVPC interactions. It is also instructive to interpret these bounds in terms of the mass scale, Λ_{TVPC} . To that end, we adopt the parameterization of Eqs. (34, 35) and present constraints in terms of Λ_{TVPC} and κ .

In what follows, we use experimental d_e and d_n limits directly as well as the limits on \bar{g}_ρ and the $\bar{g}_\pi^{(a)}$ derived from several sources. The corresponding limits on these quantities are given in Tables 1 and 2. It is also useful to convert our expressions for \bar{g}_ρ and the $\bar{g}_\pi^{(a)}$ into numerical form. In the case of \bar{g}_ρ we have

$$\bar{g}_\rho \approx -C_{7a}^{ud} (M_Z/\Lambda_{TVPC})^3 \times (2 \times 10^{-10}) \quad . \quad (95)$$

Similarly, the combinations of the $\bar{g}_\pi^{(a)}$ relevant to d_n and $d_A(^{199}\text{Hg})$ are, respectively,

$$\bar{g}_\pi^{(2)} - \bar{g}_\pi^{(0)} \approx -C_{7a} (M_Z/\Lambda_{TVPC})^3 \times (6 \times 10^{-12}) \quad (96)$$

for d_n and

$$\bar{g}_\pi^{(0)} + \bar{g}_\pi^{(1)} + 2\bar{g}_\pi^{(2)} \approx -C_{7a}^{ud} (M_Z/\Lambda_{TVPC})^3 \times (3 \times 10^{-11}) \quad (97)$$

for $d_A(^{199}\text{Hg})$.

Scenario A. Under this scenario, the first two terms in Eq. (1) vanish, so that the leading terms in the expansion of the EDM are the $\mathcal{O}(1/\Lambda_{TVPC}^3)$ contributions from the TVPC operators. As in the case of the effective hadronic

couplings, it is useful to express our relationships between the EDM's and the TVPC interactions in numerical form.

For the elementary fermion EDM's arising from the one-loop graphs containing $\mathcal{O}_{7c}^{Z\gamma}$ (Fig. 2), we require a choice for μ . Since the typical momentum of a quark in the neutron is $\sim \Lambda_{QCD}$, we take $\mu = \Lambda_{QCD}$. The appropriate choice for d_e is probably smaller, on the order of the typical momentum of an electron bound in a heavy atom. Since the μ -dependence of d_f is only logarithmic, however, the precise choice of scale is not decisive. To be conservative, we also use $\mu = \Lambda_{QCD}$ for d_e . The corresponding results are

$$\frac{d_e}{e} \sim C_{7c}^{Z\gamma} (M_Z/\Lambda_{TVPC})^3 \times (4 \times 10^{-17} \text{ cm}) \quad (98)$$

$$\begin{aligned} &\sim C_{7a}^{ff'} (4\pi\alpha/s_w)(M_Z/\Lambda_{TVPC})^3 \times (4 \times 10^{-17} \text{ cm}) \\ &\approx C_{7a}^{ff'} (M_Z/\Lambda_{TVPC})^3 \times (8 \times 10^{-18} \text{ cm}) \end{aligned} \quad (99)$$

and

$$\begin{aligned} \frac{d_n}{e} &\sim \left(\frac{4}{3}g_A^d - \frac{1}{3}g_A^u\right) \times (0.88) \times \frac{d_e}{e} \\ &\approx C_{7c}^{Z\gamma} (M_Z/\Lambda_{TVPC})^3 \times (6 \times 10^{-17} \text{ cm}) \\ &\sim C_{7a}^{ff'} (M_Z/\Lambda_{TVPC})^3 \times (1 \times 10^{-17} \text{ cm}) \quad , \end{aligned} \quad (100)$$

where we have used the naturalness relation of Eq. (35) to express $C_{7c}^{Z\gamma}$ in terms of $C_{7a}^{ff'}$ and where the 0.88 factor in Eq. (100) is the value of the bag model integral in Eqs. (47) and (50). Since the two-loop effects involving $\mathcal{O}_{7a}^{ff'}$ are suppressed relative to the one-loop $\mathcal{O}_{7c}^{Z\gamma}$ contributions, we do not give explicit numerical formulae for the former.

For the contribution to d_n from the TVPV γ -four quark interaction of Fig. 4b, generated by the loops of Fig. 5b, we find

$$\frac{d_n}{e} \sim C_{7a}^{ud} (M_Z/\Lambda_{TVPC})^3 \times (5 \times 10^{-25} \text{ cm}) \quad , \quad (101)$$

while the process of Fig. 9 yields

$$\frac{d_n}{e} \sim C_{7a}^{ff'} (M_Z/\Lambda_{TVPC})^3 \times (4 \times 10^{-28} \text{ cm}) \quad , \quad (102)$$

where we have again used Eq. (35).

We now apply these expressions to the experimental limits given in Tables 1 and 2. The results are listed in Table 3. Clearly, the one-loop elementary fermion EDM's generated by radiative corrections to $\mathcal{O}_{7c}^{Z\gamma}$ yield the most stringent bounds on Λ_{TVPC} . Whether one uses d_n or d_e , the lower bounds generated by this mechanism are roughly three orders of magnitude larger than those obtained from the many-quark effects. The reason for this difference is clear. The one-loop graphs are dominated by high-momentum ($p \sim M_Z$) intermediate states, whereas the many-quark matrix elements are governed by physics at scales $p \sim \Lambda_{QCD}$. Since the dimension of the TVPC operators is greater than that of the EDM by two, the EDM must contain at least two powers of the relevant mass scale. Hence, the one-loop $\mathcal{O}_{7c}^{Z\gamma}$ effects should be at least $(M_Z/\Lambda_{QCD})^2 \sim 2 \times 10^5$ larger than the many-quark effects in d_n .

We emphasize the comparison between the one-loop elementary fermion EDM limits and those obtained from $d_A(^{199}\text{Hg})$. In the latter case, the strongest bounds are derived from the combination of the $\bar{g}_\pi^{(a)}$ appearing in Eq. (97). Since these couplings scale as $1/\Lambda_{TVPC}^3$, one would require an improvement of nine orders of magnitude in the experimental limits on $d_A(^{199}\text{Hg})$ in order for the atomic EDM to compete with d_e and d_n ⁷. We also note that were it not for the one-loop elementary fermion limits, the diagrams of Fig. 5b – required by gauge invariance but omitted in Ref. [16] – would yield the most stringent constraints on new TVPC interactions under scenario (A). By far the weakest bounds follow from the extraction of \bar{g}_ρ from $d_A(^{199}\text{Hg})$.

The limits in Table 3 can be translated into an expectation for α_T under Scenario (A). Using the general scaling arguments of Ref. [18] which imply

$$\alpha_T \sim C_{7a}^{ff'} \left(\frac{p}{\Lambda_{TVPC}} \right)^3 = C_{7a}^{ff'} \left(\frac{M_Z}{\Lambda_{TVPC}} \right)^3 \left(\frac{p}{M_Z} \right)^3 \quad (103)$$

and using the naturalness assumption of Eq. (35) we have

$$\alpha_T \sim (7 \times 10^{-16}) \times \left(\frac{p}{1 \text{ GeV}} \right)^3. \quad (104)$$

⁷An improvement of this magnitude, however, would likely render the atomic EDM as the most precise probe of d_n .

For a low energy TVPC process with $p \sim 1$ GeV, the Scenario (A) EDM limits of Table 3 imply that the size of the effect should be roughly 10^{-15} . Current direct search limits are at the 10^{-3} level for α_T .

Scenario B. As argued above, experimental EDM limits do not apply to TVPC interactions when PV persists at short distances. In this case, one must rely on direct TVPC tests, from which limits on \bar{g}_ρ may be extracted. The most precise determinations of \bar{g}_ρ from TVPC observables are obtained from charge symmetry breaking (CSB) terms in np scattering cross sections [12] and fivefold correlations (FC) in the transmission of polarized neutrons through spin aligned Holmium [10]. The limits on \bar{g}_ρ obtained from these observables are given in Table 2. In addition, a proton-deuteron transmission experiment proposed for COSY would be sensitive to \bar{g}_ρ at the 10^{-3} level [13]. Further improvements in the np CSB limits may also be possible [14].

The bounds on Λ_{TVPC} from direct TVPC searches are given in Table 4. At present, the data imply new TVPC physics could arise at scales as light as a few GeV. Ideally, future experiments would push these bounds closer to the weak scale. Such a sensitivity would be comparable to the present and anticipated new physics sensitivities of atomic PV and PV electron scattering experiments [4]. Achieving such sensitivity, however, would be a daunting task, requiring at least six orders of magnitude improvement in precision beyond the present state of the art.

7 Conclusions

Measurements of EDM's provide one of the most powerful probes of possible new physics. Thus far, null results for d_e , d_n , and d_A lead to tight constraints on a variety of new physics scenarios. In this paper, we have studied the implications of EDM's for TVPC new physics. We have also developed relationships between effective TVPC and TVPV hadronic couplings, on the one hand, and TVPC interactions involving quarks and gauge bosons, on the other. This relationship has not been systematically delineated in the past. Consequently, some confusion about the respective implications of EDM's and the values of hadronic couplings extracted from direct TVPC searches has ensued. We believe that our analysis has helped clarify these implications.

While the possible origin of TVPC interactions in the context of a renormalizable gauge theory has yet to be delineated, one may, nevertheless, address the issue using the framework of EFT. This framework affords a systematic method for treating nonrenormalizable interactions and for carrying out the associated phenomenology. Since the operators we have treated here have $d > 4$, EFT is the natural framework for performing our analysis. As emphasized above, a key ingredient in the application of EFT to this problem is the maintenance of a scale separation. The short-distance ($p \gtrsim \Lambda_{TVPC}$) TVPC physics about which we are ignorant is parameterized by the *a priori* unknown coefficients of the nonrenormalizable effective interactions. Long distance ($p \ll \Lambda_{TVPC}$) physics may be treated explicitly in the guise of loops and many-body matrix elements involving degrees of freedom having masses and momenta below Λ_{TVPC} . As we illustrated for the example of the cut-off regulator used in the loop calculations of Refs. [16, 17], a failure to adhere to this scale separation can lead to disastrous results. Indeed, in that example, the blurring of scale separation implies (erroneously) that the EDM is proportional to an infinite series of unknown coefficients of nonrenormalizable operators of arbitrarily high dimension. Without the truncation scheme implied by the EFT scale separation, one is unable to learn anything from experiment about a given TVPC interaction (or even finite set of such interactions).

As argued at the outset of our paper, the EFT scale separation implies one must consider the low-energy consequences of TVPC new physics under two scenarios: parity-restoration below Λ_{TVPC} (Scenario A) and parity-restoration above Λ_{TVPC} (Scenario B). In the case of Scenario A, the EDM is dominated by PV radiative corrections to $d = 7$ TVPC operators. The most significant impact arises from the EDM of elementary fermions, generated by a one-loop graph involving $\mathcal{O}_{7C}^{Z\gamma}$. Interpreted in terms of a mass scale, this mechanism, taken with the experimental limits on d_e and d_n , imply that $\Lambda_{TVPC} \gtrsim 100\text{-}250$ TeV when the TVPC new physics is “strong” ($\kappa \sim 1$). The impact of many-quark effects – which contribute both directly to d_n as well as to both d_n and $d_A(^{199}\text{Hg})$ via the couplings \bar{g}_ρ and $\bar{g}_\pi^{(I)^\prime}$ – is considerably smaller than that of the one-loop elementary fermion EDM. Indeed, for the many-quark mechanism to compete with that of the elementary fermion EDM, one would require an improvement in the limits on $d_A(^{199}\text{Hg})$ of nine orders of magnitude. The impact of direct search limits is even weaker under this scenario. We conclude, then, that d_e and d_n provide the most power-

ful probes of new TVPC physics when parity symmetry is restored at short distances, while the atomic EDM measurements are better suited to constraining other new physics scenarios.

Under Scenario B, the implications of EDM's are ambiguous at best. The existence of parity-violation at short distances implies that $d \leq 7$ TVPV operators contribute to the EDM along with the radiatively corrected $d \geq 7$ TVPC operators. Consequently, no single TVPV observable constrains the latter unless one invokes additional assumptions. In contrast, the relationship between TVPC observables – such as CSB np scattering cross sections or FC in neutron transmission – is not clouded by the additional unknown constants which enter the EDM. In this case, however, the limits obtained from direct TVPC searches are rather weak: $\Lambda_{TVPC} \gtrsim 1$ GeV (for $\kappa \sim 1$). As a long term benchmark, one would ideally search for new TVPC physics at least up to the weak scale. Achieving this goal would require an improvement in the precision of direct TVPC searches by six orders of magnitude. While achieving such improvement would seem formidable, any intermediate progress would constitute a welcome step.

Acknowledgement

It is a pleasure to thank D. DeMille, R. Springer, and M. Savage, and Wim van Oers for useful discussions. This work was supported in part under U.S. Department of Energy contracts #DE-AC05-84ER40150 and #DE-FG06-90ER40561, and #DE-FG02-00ER41146 and a National Science Foundation Young Investigator Award.

References

- [1] The Particle Data Group, Euro. Phys. Journal **C15**, 1 (2000).
- [2] S.C. Bennett and C.E. Wieman, Phys. Rev. Lett. **82**, 2484 (1999); C.S. Wood *et al.*, Science **275**, 1759 (1997).
- [3] A. Derevianko, Phys. Rev. Lett. **85**, 1618 (2000).
- [4] M.J. Ramsey-Musolf, Phys. Rev. **C60**, 015501 (1999).

- [5] M.J. Ramsey-Musolf, Phys. Rev. **D62**, 056009 (2000).
- [6] A. Angelopoulos *et al.* (CPLEAR Collaboration), Phys. Lett. **B444**, 43 (1998).
- [7] E. Blanke *et al.*, Phys. Rev. Lett. **51**, 355 (1983).
- [8] F. Boehm in *Fundamental Interactions in Nuclei*, W. Haxton and E. Haxton, Eds. (World Scientific, Singapore, 1995) p. 67.
- [9] P. Herczeg, J. Kambor, M. Simonius, “Parity conserving time reversal violation in flavor conserving quark-quark interactions”, Los Alamos Theory Division report (unpublished); P. Herczeg, Hyp. Interact. **75** (1992) 127; P. Herczeg in *Fundamental Interactions in Nuclei*, W. Haxton and E. Haxton, Eds. (World Scientific, Singapore, 1995) p. 89.
- [10] P.R. Huffman *et al.*, Phys. Rev. **C55**, 2684 (1997).
- [11] J.E. Koester *et al.*, Phys. Lett. **B267**, 23 (1991).
- [12] M. Simonius, Pys. Rev. Lett. **78**, 4161 (1997).
- [13] COSY Proposal, P.D. Eversheim, spokesperson; F. Hinterberger (for the TRI Collaboration at COSY), Contribution to the Fifth Annual WEIN Symposium: A Conference on Physics Beyond the Standard Model, nucl-ex/9810013.
- [14] W.T.H. van Oers, hep-ph/9912454, to appear in Int. J. Mod. Phys. **E**.
- [15] L.J. Lising *et al.* (emiT Collaboration), Phys. Rev. **C62**, 055501 (2000).
- [16] I.B. Khriplovich, Nucl. Phys. **B352** (1991) 385.
- [17] R.S. Conti and I.B. Khriplovich, Phys. Rev. Lett. **68** (1992) 3262.
- [18] J. Engel, P.H. Frampton, R.P. Springer, Phys. Rev. **D53** (1996) 5112.
- [19] P. Herczeg, “Time reversal violation in nuclear processes”, in *Symmetries and Fundamental Interactions in Nuclei*, W.C. Haxton and E.M. Henley, eds., World Scientific, Singapore, pp. 89-126.

- [20] M.J. Ramsey-Musolf, Phys. Rev. Lett. **83**, 3997 (1999); (E) *ibid* **84** 5681 (2000).
- [21] M.J. Ramsey-Musolf, hep-ph/0010023, to appear in proceedings of the Workshop on Fundamental Physics with Pulsed Neutron Beams, Durham, N.C., May, 2000.
- [22] M.J. Ramsey-Musolf and H. Ito, Phys. Rev. **C55**, (3066).
- [23] C. Itzykson and J.-B. Zuber, Quantum Field Theory, McGraw-Hill, New York, 1980.
- [24] Note that the result in Eq. (31) is a factor of six larger than Eq. (6) of Ref. [20], which contains an error.
- [25] J.F. Donoghue, E. Golowich, and B. Holstein, Phys. Rep. **131**, 319 (1986).
- [26] Sakuri, J. J., Currents and Mesons, University of Chicago press, Chicago, 1969.
- [27] W. C. Haxton, A. Horing, and M. J. Ramsey-Musolf, Phys Rev **D50** 3422.
- [28] W.M. Snow *et al.*, Nucl. Inst. Meth. **A440**, 729 (2000).
- [29] K. F. Smith *et al.* Phys. Lett. **B234** (1990) 191, I. S. Altev *et al.* Phys. Lett. **B276** (1992) 242, P. G. Harris *et al.* Phys. Rev. Lett. **82** (1999) 904.
- [30] R.H. Crewther, P. Di Vecchia, G. Veneziano, and E. Witten, Phys. Lett. **B88**, 123 (1979); *ibid* **91**, 487 (E) (1980).
- [31] G. Barton and E.G. White, Phys. Rev. **184**, 1660 (1969).
- [32] G. Valencia, Phys. Rev. **D41**, 1562 (1990).
- [33] X-G. He and B. McKellar, Phys. Rev. **D47**, 4055 (1993).
- [34] E.D. Commins *et al.*, Phys. Rev. **A50**, 2960 (1994).

- [35] B. Desplanques, J.F. Donoghue, and B. Holstein, *Ann. Phys. (NY)* **124**, 449 (1980).
- [36] J.P. Jacobs *et al.* *Phys. Rev.* **A52**, 3521 (1995).

A Quark model matrix elements

Here, we evaluate the matrix elements appearing in Eq. (57). We define the following quantities: $P = p_N + p_P$, $q = p_\rho = p_N - p_P$, ϵ is the ρ polarisation. Since the TVPC ρNN Lagrangian is linear in the ρ momentum operator, we retain only those terms in the matrix element products linear in q . The fourth matrix element product in Eq. (57) is quadratic in q since the nucleon matrix element vanishes to first order in q . Thus, the last product does not contribute to \bar{g}_ρ .

For the remaining matrix element products in Eq. (57), we first require the ρ to vacuum matrix element, parameterized in the standard way as

$$\langle 0 | \bar{u} \gamma_\mu d | \rho^- \rangle = \sqrt{2} \frac{m_\rho^2}{f_\rho} \epsilon_\mu e^{i\vec{p} \cdot \vec{x}} \quad (105)$$

where $f_\rho^2/4\pi \approx 2.5$. The rho matrix element with the derivative may be evaluated using wave packets in the quark model, using the approach of Donoghue and Johnson [25]. We begin by assuming the following structure for the matrix element,

$$\langle 0 | \bar{u} \overleftarrow{\partial}_\mu d | \rho^- \rangle = (a\epsilon_\mu + bp_\mu) e^{ipx} \quad (106)$$

where p_μ is the momentum of the rho-meson and ϵ_μ is the polarization vector. We solve for the coefficients, a and b . The quark model matrix element may be written using wave packets as

$$\langle 0 | \bar{u} \overleftarrow{\partial}_\mu d | \rho^- \rangle_{QM} = \int \frac{d^3 p'}{2\omega_{p'}} \phi(p') \langle 0 | \bar{u} \overleftarrow{\partial}_\mu d | \rho^- \rangle \quad (107)$$

Multiplying each side of the equation by $\int d^3 x \exp(-i\vec{p} \cdot \vec{x}) / (2\pi)^3$, results in

$$\int \frac{d^3 x}{(2\pi)^3} \exp(-i\vec{p} \cdot \vec{x}) \langle 0 | \bar{u} \overleftarrow{\partial}_\mu d | \rho^- \rangle_{QM} = \frac{\phi(p)}{2\omega_p} (a\epsilon_\mu + bp_\mu). \quad (108)$$

The expression for $\phi(p)$ may be obtained from the vector current matrix element Eq. (105),

$$\int \frac{d^3 x}{(2\pi)^3} \exp(-i\vec{p} \cdot \vec{x}) \langle 0 | \bar{u} \gamma_\mu d | \rho^- \rangle_{QM} = \phi(p) \frac{\epsilon_\mu m_\rho^2}{f_\rho \omega_p \sqrt{2}} \quad (109)$$

We use the $\mu = 3$ component of the above equation to find an expression for $\phi(p)$. This, taken together with the vector current matrix element produces,

$$\int d^3x e^{-i\vec{p}\cdot\vec{x}} \langle 0 | \bar{u} \overleftarrow{\partial}_\mu d | \rho^- \rangle_{QM} = \sqrt{2} f_\rho (a \epsilon_\mu + b p_\mu) \int d^3x e^{-i\vec{p}\cdot\vec{x}} \langle 0 | \bar{u} \gamma_3 d | \rho^- \rangle_{QM} \quad (110)$$

Upon evaluating both quark model matrix elements, we find $b = 0$, while,

$$a = \frac{m_\rho^2}{f_\rho} \frac{2}{3} \int \left[\frac{du}{dr} l - 2ul/r - u \frac{dl}{dr} \right] r^2 dr / \int (u^2 - l^2/3) r^2 dr. \quad (111)$$

Here, u and l are the upper and lower components of the Quark Model wave functions, respectively. The final expression is

$$\langle 0 | \bar{u} \overleftarrow{\partial}_\mu d | \rho^- \rangle = -\frac{1.05}{R_\rho} \sqrt{2} \frac{m_\rho^2}{f_\rho} i \epsilon_\mu e^{-i\vec{p}\cdot\vec{x}}. \quad (112)$$

In this expression, $R_\rho = 3.3 - 3.5 \text{ GeV}^{-1}$ is the radius of the rho meson in the bag model. In the following we shall also use $R_n = 1 \text{ fm}$ for the bag model radius of the nucleon. The nucleon matrix elements also may be evaluated with the quark model.

$$\langle n | \bar{d} \gamma_\mu u | p \rangle = \bar{u}_n (\gamma^\mu + 0.168 i R_n \sigma^{\mu\nu} q_\nu) u_p. \quad (113)$$

$$\langle n | \bar{d} \overrightarrow{\partial}_\nu u | p \rangle = 0.634 i \omega \bar{u}_n \gamma_\nu u_p \quad (114)$$

where $\omega = 2.04/R_n$ is quark energy inside the bag.

For the third matrix element product, we obtain using similar methods and Eqs. (48, 49)

$$\begin{aligned} \frac{1}{2} \langle 0 | \bar{u} (\overleftarrow{\partial}_\mu \gamma_\nu - \overleftarrow{\partial}_\nu \gamma_\mu) d | \rho^- \rangle &= i \frac{5 + 3g_A}{15 + 3g_A} \frac{m_\rho^2}{2^{1/2} f_\rho} (\epsilon_\nu q_\mu - \epsilon_\mu q_\nu) \\ \langle n | \bar{d} \sigma^{\mu\nu} u | p \rangle &= \frac{5}{12} \left(1 + \frac{g_A}{5} \right) \bar{u}_N \sigma^{\mu\nu} u_P + \dots, \end{aligned}$$

where the $+\dots$ denote terms higher order in q .

B Fierz transformed four-quark operators

In calculating the TVPV π^\pm -nucleon couplings, we require the Fierz transformed form of the amplitude in Eq. (46). The transformed amplitude is

$$\begin{aligned}
\mathcal{M}_5^{FIERZ} = & \frac{C_{7a}^{ff'}}{\Lambda_{TVP}^3} \frac{\alpha}{32\pi s_W^2 c_W^2} \log\left(\frac{\mu^2}{M_Z^2}\right) \{ \\
& im_{f'} \left(4g_A^{f'} g_V^f - \frac{1}{2}g_V^f g_A^f\right) (\bar{U}_f \gamma_5 U_{f'} \bar{U}_{f'} U_f + \bar{U}_f U_{f'} \bar{U}_{f'} \gamma_5 U_f) \\
& + im_{f'} \left(2g_A^{f'} g_V^f + \frac{1}{2}g_V^f g_A^f\right) (\bar{U}_f \gamma_\mu U_{f'} \bar{U}_{f'} \gamma^\mu \gamma_5 U_f - \bar{U}_f \gamma_\mu \gamma_5 U_{f'} \bar{U}_{f'} \gamma^\mu U_f) \\
& - \frac{i}{4} m_{f'} g_V^f (g_A^f + g_A^{f'}) \bar{U}_f \sigma^{\mu\nu} U_{f'} \bar{U}_{f'} \gamma_5 \sigma_{\mu\nu} U_f + \frac{i}{4} m_{f'} g_V^f g_A^{f'} \bar{U}_f \gamma_5 \sigma^{\mu\nu} U_{f'} \bar{U}_{f'} \sigma_{\mu\nu} U_f \\
& + i(p'_{f'} + p_f)^\mu (2g_A^{f'} g_V^{f'} - g_V^{f'} g_A^f + \frac{7}{2}g_A^f g_V^{f'}) \frac{1}{4} (\bar{U}_f U_{f'} \bar{U}_{f'} \gamma_\mu \gamma^5 U_f - \bar{U}_f \gamma_\mu \gamma_5 U_{f'} \bar{U}_{f'} U_f) \\
& + i(p'_{f'} + p_f)^\mu (2g_A^{f'} g_V^{f'} - g_V^{f'} g_A^f + \frac{7}{2}g_A^f g_V^{f'}) \frac{1}{4} (\bar{U}_f \gamma_5 U_{f'} \bar{U}_{f'} \gamma_\mu U_f + \bar{U}_f \gamma_\mu U_{f'} \bar{U}_{f'} \gamma_5 U_f) \\
& - (p'_{f'} + p_f)^\mu (2g_A^{f'} g_V^{f'} - g_V^{f'} g_A^f + \frac{7}{2}g_A^f g_V^{f'}) \frac{1}{4} (\bar{U}_f \sigma_{\mu\nu} \gamma_5 U_{f'} \bar{U}_{f'} \gamma^\nu U_f - \bar{U}_f \gamma^\nu U_{f'} \bar{U}_{f'} \sigma_{\mu\nu} \gamma_5 U_f) \\
& - (p'_{f'} + p_f)^\mu (2g_A^{f'} g_V^{f'} - g_V^{f'} g_A^f + \frac{7}{2}g_A^f g_V^{f'}) \frac{1}{4} (\bar{U}_f \gamma^\nu \gamma_5 U_{f'} \bar{U}_{f'} \sigma_{\mu\nu} U_f + \bar{U}_f \sigma_{\mu\nu} U_{f'} \bar{U}_{f'} \gamma^\nu \gamma_5 U_f) \\
& + \frac{3}{8} g_A^f g_V^{f'} i(p'_{f'} + p_{f'})_\mu (\bar{U}_f \gamma_\mu U_{f'} \bar{U}_{f'} \gamma_5 U_f + \bar{U}_f \gamma_5 U_{f'} \bar{U}_{f'} \gamma_\mu U_f) \\
& - \frac{3}{8} g_A^f g_V^{f'} i(p'_{f'} + p_{f'})_\mu (\bar{U}_f \gamma_\mu \gamma_5 U_{f'} \bar{U}_{f'} U_f - \bar{U}_f U_{f'} \bar{U}_{f'} \gamma_\mu \gamma_5 U_f) \\
& - \frac{1}{8} g_A^f g_V^{f'} (p'_{f'} + p_{f'})_\mu (\bar{U}_f \sigma_{\nu\mu} U_{f'} \bar{U}_{f'} \gamma_\nu \gamma_5 U_f + \bar{U}_f \gamma_\nu \gamma_5 U_{f'} \bar{U}_{f'} \sigma_{\nu\mu} U_f) \\
& + \frac{1}{8} g_A^f g_V^{f'} (p'_{f'} + p_{f'})_\mu (\bar{U}_f \gamma_\nu U_{f'} \bar{U}_{f'} \gamma_5 \sigma_{\nu\mu} U_f - \bar{U}_f \gamma_5 \sigma_{\nu\mu} U_{f'} \bar{U}_{f'} \gamma_\nu U_f) \} \tag{115}
\end{aligned}$$

Only the first two terms on the RHS of Eq. (115) contribute in the factorization approximation. The terms on the second line, such as $\bar{U}_f \gamma_\mu U_{f'} \bar{U}_{f'} \gamma^\mu \gamma_5 U_f$ will not contribute in this approximation. The reason is that the pion-to-vacuum matrix element will be proportional to the pion momentum, q , which equals the change of the momentum of the nucleon. When contracted with the nucleon matrix element of the vector current, the result vanishes by current conservation (neglecting the small n - p mass difference). The terms on the third line will not contribute for symmetry reasons.

The remaining terms involve derivatives on the quark fields. In each case the derivative pair is split, so one derivative acts on a quark field in one quark bilinear and the second derivative acts on the second. Some of these terms may be rewritten using equations of motion for the on shell quarks. Doing so yields new contributions to the first four lines of the RHS of Eq. (115), requiring an adjustment in the coefficients. The remaining terms involve derivative operators, such as

$$\bar{U}_f p'_{f\mu} U_{f'} \bar{U}_{f'} \gamma^\mu \gamma_5 U_f \quad \text{and} \quad \bar{U}^f p'_{f\mu} \gamma^5 U_{f'} \bar{U}_{f'} \gamma^\mu U_f. \quad (116)$$

Factorization matrix elements of these operators vanish by either symmetry or current conservation.

Finally, tensor structures such as $\bar{U}^f p'_{f\mu} \gamma_\nu U_{f'} \bar{U}_{f'} \sigma^{\mu\nu} \gamma_5 U_f$ cannot produce a pion-vacuum matrix element, while those such as $\bar{U}_f p'_{f\mu} \gamma_\nu \gamma_5 U_{f'} \bar{U}_{f'} \sigma^{\mu\nu} U_f$ will vanish from symmetry considerations.

Table 1: Present experimental limits on electric dipole moments.

| Observable | Experimental limit (e-cm) | Ref. |
|------------------------|----------------------------|------|
| d_e | $\leq 4 \times 10^{-27}$ | [34] |
| d_n | $\leq 8 \times 10^{-26}$ | [29] |
| $d_A(^{199}\text{Hg})$ | $\leq 1.3 \times 10^{-27}$ | [36] |

Table 2: Experimental limits on TVPC and TVPV hadronic couplings. The value of $h_{\pi NN}^{DDH}$ is the “best value give in Ref. [35].

| Coupling | Experimental limit | Observable |
|--|--|------------------------------------|
| \bar{g}_ρ | $\leq 9.3 \times 10^{-3}$ | $d_A(^{199}\text{Hg})$ & atomic PV |
| \bar{g}_ρ | $\leq 0.53 \times 10^{-3} (h_{\pi NN}^{DDH}/h_{\pi NN})$ | d_n |
| \bar{g}_ρ | $\leq 5.8 \times 10^{-2}$ | FC in neutron transmission |
| \bar{g}_ρ | $\leq 6.7 \times 10^{-3}$ | CSB in np scattering |
| $ \bar{g}_\pi^{(2)} - \bar{g}_\pi^{(0)} $ | $\leq 5.7 \times 10^{-12}$ | d_n |
| $ \bar{g}_\pi^{(0)} + \bar{g}_\pi^{(1)} + 2\bar{g}_\pi^{(2)} $ | $\leq 1.8 \times 10^{-11}$ | $d_A(^{199}\text{Hg})$ |

Table 3: Limits on new TVPC interactions derived from EDM’s under Scenario (A).

| Observable | Lower bound on $\Lambda_{TVPC}/k^{2/3}$ (TeV) | Mechanism |
|------------------------|---|---|
| d_e | 260 | single electron $\mathcal{O}_{7c}^{Z\gamma}$ loop |
| d_n | 110 | single quark $\mathcal{O}_{7c}^{Z\gamma}$ loop |
| d_n | 0.39 | Figs. 4b, 5b |
| d_n | 0.21 | π -loop, Fig. 8b |
| d_n | 0.036 | Fig. 9 |
| $d_A(^{199}\text{Hg})$ | 0.25 | $\bar{g}_\pi^{(a)}$ (Fig. 1c) |
| $d_A(^{199}\text{Hg})$ | 0.0006 | \bar{g}_ρ , atomic PV (Fig. 1b) |

Table 4: Limits on new TVPC interactions derived from direct searches under Scenario (B).

| Coupling | Lower bound on $\Lambda_{TVPC}/\kappa^{2/3}$ (TeV) | Observable |
|----------------|--|----------------------------|
| \bar{g}_ρ | 3×10^{-4} | CSB in np scattering |
| \bar{g}_ρ | 7×10^{-4} | FC in neutron transmission |

Figure 1: Representative contributions to atomic EDM: (a) TVPV nuclear effect involving TVPC and PV ρNN interactions; (b) TVPC nuclear effect plus atomic PV; (c) long-range TVPV nuclear effect involving TVPV πNN coupling. Open circle denotes strong meson-nucleon coupling; crossed circle gives TVPC coupling; open square is TCPV coupling; and crossed square is TVPV coupling.

Figure 2: One loop contribution to elementary fermion EDM from the TVPC operator $\mathcal{O}_7^{\gamma Z}$. Coupling symbols are as in Fig. 1.

Figure 3: Two loop contributions to the elementary fermion EDM involving the TVPC operator $\mathcal{O}_7^{ff'}$. Symbols are as in Fig. 1.

Figure 4: Contributions from four-quark TVPV operators to d_n : (a) second order contribution involving a mixture of opposite parity states $|n\rangle$ into neutron; (b) first-order contribution arising from γ -four quark TVPV operators. Symbols are as in Fig. 1.

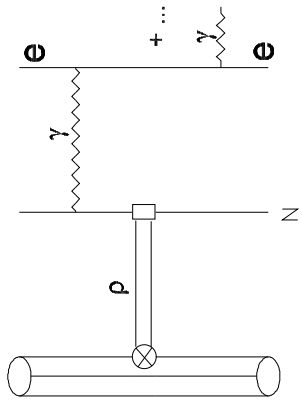
Figure 5: PV weak radiative corrections to $\mathcal{O}_{7a}^{ff'}$, generating $d = 7$ TVPV operators. Symbols are as in Fig. 1.

Figure 6: Contribution to d_n from individual quark EDM's. Symbols are as in Fig. 1.

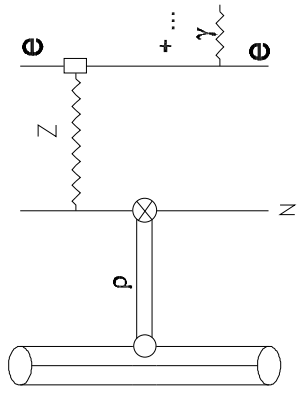
Figure 7: (a) Contributions to \bar{g}_ρ from $\mathcal{O}_{7a}^{ff'}$; (b) contribution to d_n arising from TVPC ρNN and PV πNN interactions. Symbols are as in Fig. 1.

Figure 8: (a) Contributions to $\bar{g}_\pi^{(I) \prime}$ arising from TVPV many-quark operators; (b) leading-order contribution (in m_π) to d_n arising from TVPV πNN interaction. Symbols are as in Fig. 1.

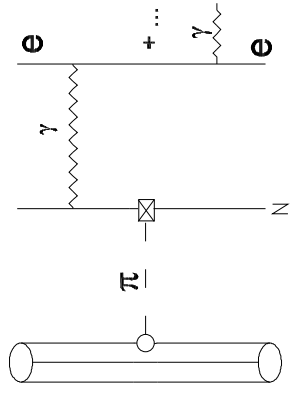
Figure 9: Tree-level, many-quark contribution to d_n generated by $\mathcal{O}_{7c}^{Z\gamma}$. Symbols are as in Fig. 1.



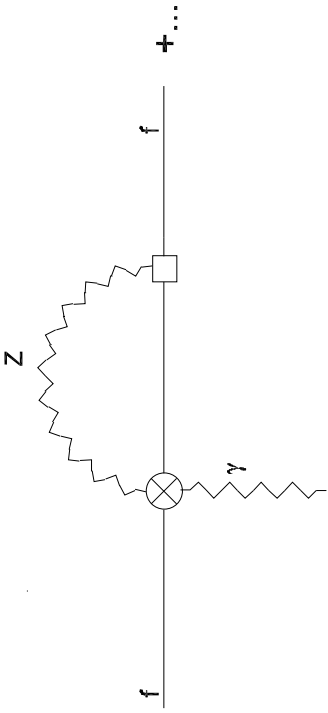
(a)

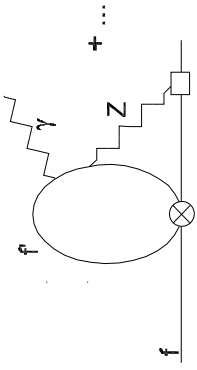


(b)

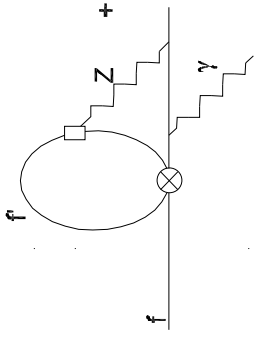


(c)

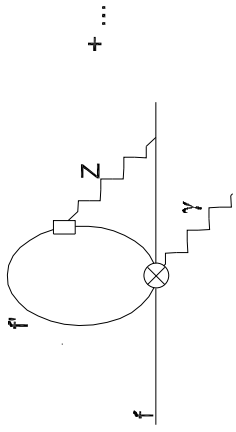




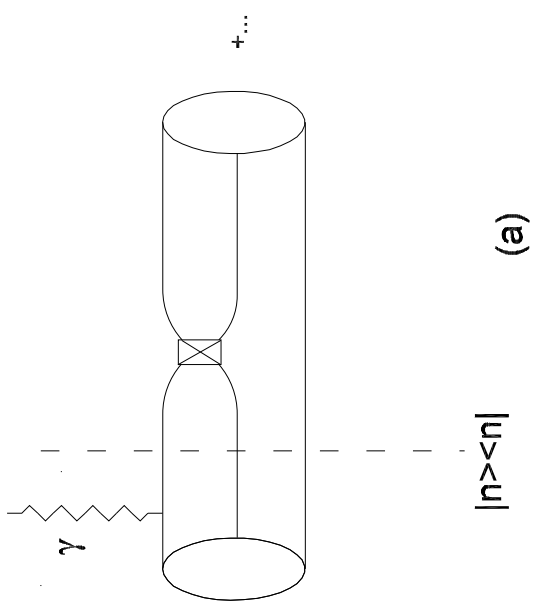
(a)



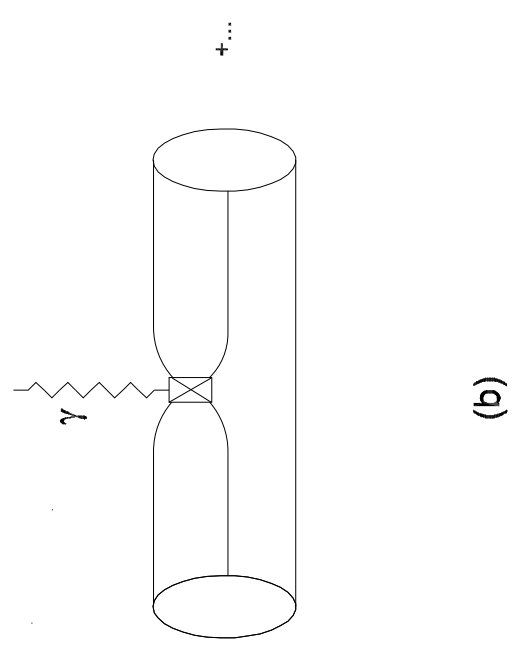
(b)



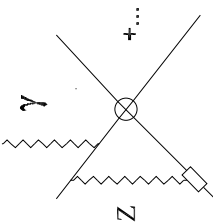
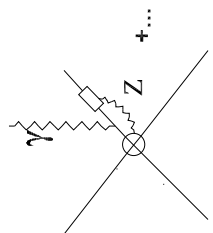
(c)



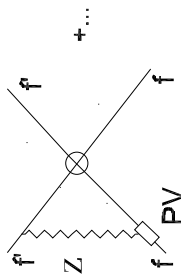
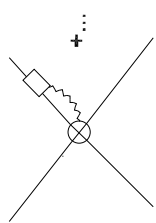
(a)



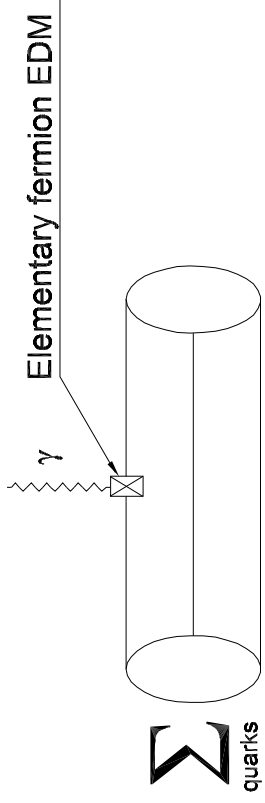
(b)

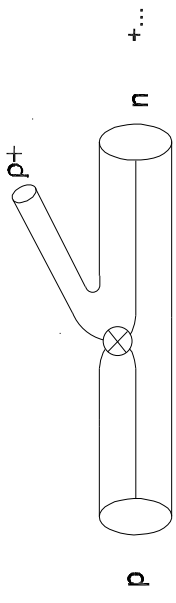


(b)

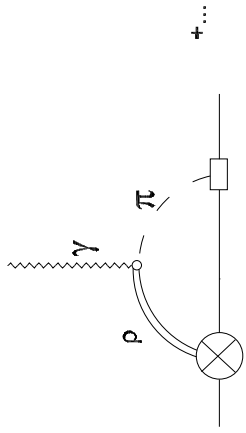


(a)

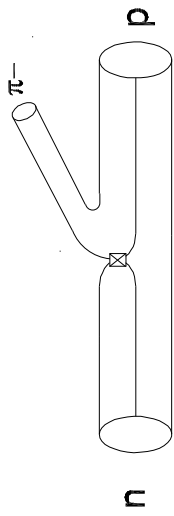




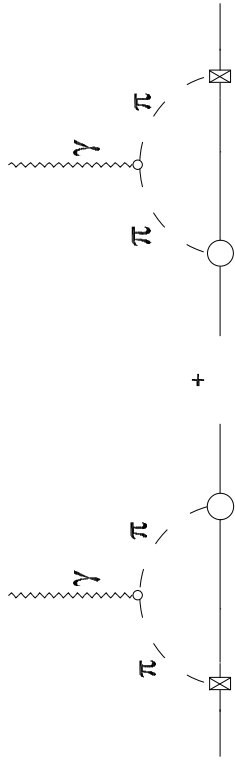
(a)



(b)



(a)



(b)

